

ANIMC: A Soft Approach for Auto-weighted Noisy and Incomplete Multi-view Clustering

Xiang Fang, Yuchong Hu, *Member, IEEE*, Pan Zhou, *Senior Member, IEEE*,
and Dapeng Oliver Wu, *Fellow, IEEE*

Abstract—Multi-view clustering has wide real-world applications because it can process data from multiple sources. However, these data often contain missing instances and noises, which are ignored by most multi-view clustering methods. Missing instances may make these methods difficult to use directly, and noises will lead to unreliable clustering results. In this paper, we propose a novel Auto-weighted Noisy and Incomplete Multi-view Clustering approach (ANIMC) via a *soft* auto-weighted strategy and a doubly *soft* regular regression model. Firstly, by designing adaptive semi-regularized nonnegative matrix factorization (adaptive semi-RNMF), the soft auto-weighted strategy assigns a *proper* weight to each view and adds a soft boundary to balance the influence of noises and incompleteness. Secondly, by proposing θ -norm, the doubly soft regularized regression model adjusts the sparsity of our model by choosing different θ . Compared with previous methods, ANIMC has three unique advantages: 1) it is a soft algorithm to adjust our approach in different scenarios, thereby improving its generalization ability; 2) it automatically learns a proper weight for each view, thereby reducing the influence of noises; 3) it performs doubly soft regularized regression that aligns the same instances in different views, thereby decreasing the impact of missing instances. Extensive experimental results demonstrate its superior advantages over other state-of-the-art methods.

Impact Statement—As an effective method to process data from multiple sources, multi-view clustering has attracted more and more attention. However, most previous works ignore missing instances and noises in original multi-view data, which limits the applications of these works. By a soft approach, our proposed ANIMC can effectively reduce the negative influence of missing instances and noises. Moreover, ANIMC outperforms the state-of-the-art works by about 20% in representative cases. With satisfactory performance on multiple real-world datasets, ANIMC has wide potential applications including the analysis of multilingual document and image datasets.

This work is supported by National Natural Science Foundation of China (NSFC) under grant no. 61972448. (*Corresponding author: Pan Zhou.*)

X. Fang is with the Hubei Engineering Research Center on Big Data Security, School of Cyber Science and Engineering Huazhong University of Science and Technology, also with the School of Computer Science and Technology, Huazhong University of Science and Technology, Wuhan 430074, China (e-mail: xfang9508@gmail.com).

Y. Hu is with the School of Computer Science and Technology, Key Laboratory of Information Storage System Ministry of Education of China, Huazhong University of Science and Technology, Wuhan 430074, China (e-mail: yuchonghu@hust.edu.cn).

P. Zhou is with the Hubei Engineering Research Center on Big Data Security, School of Cyber Science and Engineering, Huazhong University of Science and Technology, Wuhan 430074, China (e-mail: panzhou@hust.edu.cn).

D. O. Wu is with the Department of Electrical and Computer Engineering, University of Florida, Gainesville, FL 32611, USA (e-mail: dpwu@ieee.org).

© 2021 IEEE. Personal use of this material is permitted. Permission from IEEE must be obtained for all other uses, in any current or future media, including reprinting/republishing this material for advertising or promotional purposes, creating new collective works, for resale or redistribution to servers or lists, or reuse of any copyrighted component of this work in other works.

Index Terms—Noisy and incomplete multi-view clustering, Soft auto-weighted strategy, Doubly soft regularized regression.

I. INTRODUCTION

REAL-WORLD data [1]–[3] often come from different sources, which are called *multi-view data* [4]–[6]. For example, the collected images [7]–[10] can be represented by different visual descriptors (i.e., different views) [11]–[66], like CTM [67]–[69], GIST [70]–[72], SIFT [73], etc; web pages can be represented by different kinds of features based on text and hyper-links [74]–[76]. Integrating the information from different views can help us analyze the data in a comprehensive manner [74], [75], [77], which motivates multi-view clustering methods [78]–[81]. The purpose of multi-view clustering is to adaptively partition data into their respective groups by fully integrating the information from multiple views [76]. Up to the present, many multi-view clustering methods have been proposed, like space-based methods [79], [82], [83], graph-based methods [84]–[86], nonnegative matrix factorization (NMF) based methods [87], [88], etc. Although most multi-view clustering methods can solve some problems in real-world applications, they still face two major problems.

One problem is the missing instances in multi-view data [89]. Most multi-view clustering methods require that each view has no missing instances. But real-world multi-view data always contain missing instances, which leads to the incomplete multi-view clustering problem. For example, in the camera network, some cameras may temporarily fail due to a power outage, which will result in missing instances. As such, this incompleteness may lead to the lack of columns or rows in the view matrix, which will result in the degradation or failure of previous methods.

The other problem is the noises in multi-view data. For instance, real-world images often contain some noises [90]–[92]. For instance, many landscape images often contain fog and rain, which are common noises in image processing. If we directly cluster these landscape images, these noises may cause deviations in the calculation, which will damage the performance.

Up to now, there is no effective method to solve these two problems at the same time. To tackle the first problem, several incomplete multi-view clustering methods have been proposed [93]–[95]. But they ignore the influence of noises (i.e., the second problem), which are ubiquitous in the real-world clustering tasks [96], [97]. Specifically, these methods directly conduct the procedure by constructing a basis matrix for each

view and a common latent subspace for all views that are rarely modified. But real-world datasets always contain noises that result in unreliable basis matrices and unavailable latent subspace. These noises will affect the clustering calculation, which may lead to inaccurate clustering results. For the second problem, a simple solution is to assign a proper weight to each view [85], [98]–[100]. However, previous incomplete multi-view clustering methods are difficult to effectively weight different views due to the following challenges [93]–[95], [101], [102]:

- The combined effects of noises and incompleteness make these incomplete multi-view clustering methods obtain unsatisfactory clustering results. When we cluster these multi-view datasets, both missing instances and noises will influence the weights of these views. Previous methods are difficult to consider the effects of missing instances and noises simultaneously. Besides, when the missing rate and the noisy rate changes, these methods are difficult to balance this effect.
- As the missing rate increases, the availability of each view also changes. If we weigh each view based on parameters, the selection of parameters for each case will have a high cost of time and it will be difficult for us to assign a proper weight to each view. To our best knowledge, it is still an open problem to select the optimal values for these parameters in different clustering tasks, which limits the application of parameter-weighted incomplete multi-view clustering methods.
- Defined in [103], the generalization ability of clustering methods is valued by many works [104]–[106]. Strong generalization ability often means that a method can keep satisfactory performance in different datasets. To effectively cluster different data sets, we often need different objective functions. A clustering method with strong generalization ability often designs different objective functions rather than a single objective function. Thus, a series of effective objective functions should be designed to improve the generalization ability. The generalization ability of previous methods is limited because these methods are based on a single objective function. The single objective function often performs well only in some cases.

Therefore, multi-view clustering still faces significant challenges. In this paper, we propose a novel Auto-weighted Noisy and Incomplete Multi-view Clustering (ANIMC) approach to meet these challenges. ANIMC is a joint of a *soft* auto-weighted strategy and a doubly *soft* regularized regression model¹. First, by designing adaptive semi-regularized nonnegative matrix factorization (adaptive semi-RNMF), we propose a soft auto-weighted strategy to assign a *proper* weight to each view. Second, by devising θ -norm, we perform doubly soft regularized regression to align the same instances in different views. The main contributions of our proposed ANIMC approach are summarized as follows:

- To the best of our knowledge, ANIMC is the *first* auto-weighted soft approach for noisy and incomplete multi-

view clustering. The soft approach can keep high-level clustering performance on different datasets, which verifies its strong generalization ability.

- By proposing adaptive semi-RNMF, ANIMC adaptively assigns a proper weight to each view, which diminishes the effect of noises. Also, ANIMC adds a soft boundary to the soft auto-weighted strategy, which balances the influence of noises and missing instances.
- By performing a doubly soft regularized regression model based on θ -norm, ANIMC aligns the same instances in all views, which decreases the impact of missing instances. Besides, different θ can be chosen to adjust the sparsity of the model.
- Experimental results on six real-world datasets show that ANIMC significantly outperforms state-of-the-art methods. Moreover, by making the falling direction of the objective function closer to the gradient direction, ANIMC tremendously accelerates the convergence speed by a four-step alternating iteration procedure.

The rest of the paper is organized as follows. Related work is covered in Section II. The background is described in Section III. The proposed ANIMC approach is designed in Section IV. Performance evaluations are reported in Section V. We conclude the paper in Section VI.

II. RELATED WORK

Since the related work for our approach is incomplete multi-view clustering, we will review some incomplete multi-view clustering algorithms in this section. Up to now, several incomplete multi-view clustering algorithms have been proposed [93]–[95], [101], [102]. In this section, we describe some algorithms that are most relevant to our approach. Besides ignoring the influence of noises (see Section I), each of these algorithms has distinct drawbacks. These drawbacks often lead to unsatisfactory clustering results, which limits their real-world applications.

To integrate more than two incomplete views, [93] proposes MIC by filling the missing instances in each view with average feature values. After this filling, MIC can learn a common latent subspace via weighted NMF and $L_{2,1}$ -norm regularization from multiple incomplete views. However, if we cluster multi-view datasets with relatively large missing rates, this simply filling will result in unsatisfactory results. To align the instance information, [94] proposes DAIMC by extending MIC via weighted semi-NMF [107] and $L_{2,1}$ -norm regularized regression. To obtain the robust clustering results, [95] proposes UEAF by the unified common embedding aligned with incomplete views inferring approach. But DAIMC and UEAF rely too much on alignment information, which limits their application in the datasets without enough alignment information. To simultaneously clustering and imputing the incomplete base clustering matrices, [108] proposes EE-IMVC by solving the resultant optimization problem. To obtain better clustering performance, [109] proposes EE-R-IMVC by extending EE-IMVC. Both EE-IMVC and EE-R-IMVC need to learn a consensus clustering matrix from an incomplete multi-view dataset. When the dataset contains some noises,

¹A soft model is a series of functions with similar structures.

EE-IMVC and EE-R-IMVC are difficult to learn the correct consensus clustering matrix, which will limit their application. To learn the consistent information between different views and the unique information of each view, V³H decomposes each subspace into a variation matrix for the corresponding view and a heredity matrix for all the views to represent the unique information and the consistent information respectively. As the first effective method to cluster multiple views with different incompleteness, UIMC is proposed to integrate these unbalanced incomplete views for clustering.

III. BACKGROUND

For convenience, we first define some notations throughout the paper. Then, we introduce two matrix factorization methods for single-view clustering: Regularized Matrix Factorization (RMF, in Section III-A) and semi-nonnegative Matrix Factorization (semi-NMF, in Section III-B). By extending RMF and semi-NMF, we design semi-RNMF (in Section III-C) and leverage semi-RNMF for incomplete multi-view clustering (in Section III-D).

Notation: For a multi-view dataset $\{\mathbf{X}^{(v)}\}_{v=1}^m \in \mathbb{R}^{d_v \times n}$ with n instances and m views, we can cluster these instances into c clusters, where d_v is the feature dimension of the v -th view; $[n] \stackrel{\text{def}}{=} \{1, 2, \dots, n\}$; $\mathbf{U}^{(v)} \in \mathbb{R}^{d_v \times c}$ is the basis matrix of the v -th view, $\mathbf{V} \in \mathbb{R}^{n \times k}$ is the common latent feature matrix of all the views; for any matrix \mathbf{B} , $B_{i,j}$ is the element in its i -th row and j -th column, and $\mathbf{B}_{i,:}$ is its i -th row; \mathbf{I} denotes the identity matrix; $\mathbf{g}^{(v)} \in \mathbb{R}^{n \times 1}$ is an n -dimensional vector to indicate the incompleteness of the v -th view, and we diagonalize $\mathbf{g}^{(v)}$ to the diagonal matrix $\mathbf{T}^{(v)} \in \mathbb{R}^{n \times n}$; $\|\cdot\|_F$ is F-norm; $\|\cdot\|_{2,1}$ is $L_{2,1}$ -norm; $\|\cdot\|_\theta$ is θ -norm; for any number q , q^+ is its right limit; α and β are the nonnegative parameters; θ and r are the parameters adjustable as needed.

A. Regularized Matrix Factorization

As a popular latent feature learning method, regularized matrix factorization (RMF) [110]–[112] outperforms other latent feature learning methods based on KNN or co-clustering. For a data matrix $\mathbf{X} \in \mathbb{R}^{d \times n}$, RMF approximates \mathbf{X} with a matrix $\mathbf{V} \in \mathbb{R}^{n \times c}$ and a matrix $\mathbf{U} \in \mathbb{R}^{d \times c}$. Therefore, the objective function is as follows:

$$\min_{\mathbf{U}, \mathbf{V}} \|\mathbf{X} - \mathbf{UV}^T\|_F^2 + \alpha(\|\mathbf{U}\|_F^2 + \|\mathbf{V}\|_F^2), \quad (1)$$

where α is a nonnegative parameter. For ease of description, we name \mathbf{U} as the *basis matrix* and \mathbf{V} as the *latent feature matrix*.

Note that Eq. (1) is a biconvex problem. Therefore, it is unrealistic to expect an algorithm to find the global optimal solution. Similar to [110], [111], we can update \mathbf{U} and \mathbf{V} by (i) Update \mathbf{U} (while fixing \mathbf{V}) by $\mathbf{U} = \mathbf{XV}(\alpha\mathbf{I} + \mathbf{V}^T\mathbf{V})^{-1}$. (ii) Update \mathbf{V} (while fixing \mathbf{U}) by $\mathbf{V} = \mathbf{X}^T\mathbf{U}(\alpha\mathbf{I} + \mathbf{U}^T\mathbf{U})^{-1}$.

B. Semi-nonnegative Matrix Factorization

Since semi-nonnegative matrix factorization (semi-NMF) [107] can extract the latent feature information from the data, it has been widely used in single view clustering. For

a data matrix $\mathbf{X} \in \mathbb{R}^{d \times n}$, semi-NMF approximates \mathbf{X} with a nonnegative latent feature matrix $\mathbf{V} \in \mathbb{R}^{n \times c}$ and a basis matrix $\mathbf{U} \in \mathbb{R}^{d \times c}$. Since \mathbf{U} can be negative, semi-NMF can handle negative input, which extends NMF. The framework of semi-NMF is

$$\begin{aligned} & \min_{\mathbf{U}, \mathbf{V}} \|\mathbf{X} - \mathbf{UV}^T\|_F^2 \\ & \text{s.t. } \mathbf{V}_{i,j} \geq 0, i \in [n], j \in [k]. \end{aligned} \quad (2)$$

Similar to RMF, the objective function of Eq. (2) is biconvex. [107] proposes an iterative updating algorithm to find the locally optimal solution as follows:

- (i) Update \mathbf{U} (while fixing \mathbf{V}) by $\mathbf{U} = \mathbf{XV}(\mathbf{V}^T\mathbf{V})^{-1}$.
- (ii) Update \mathbf{V} (while fixing \mathbf{U}) by

$$\mathbf{V}_{i,j} = \mathbf{V}_{i,j} \cdot \sqrt{\frac{(\mathbf{X}^T\mathbf{U})_{i,j}^+ + [\mathbf{V}(\mathbf{U}^T\mathbf{U})]_{i,j}^-}{(\mathbf{X}^T\mathbf{U})_{i,j}^- + [\mathbf{V}(\mathbf{U}^T\mathbf{U})]_{i,j}^+}}, \quad (3)$$

where $\mathbf{B}_{i,j}^+ = (|\mathbf{B}_{i,j}| + \mathbf{B}_{i,j})/2$, $\mathbf{B}_{i,j}^- = (|\mathbf{B}_{i,j}| - \mathbf{B}_{i,j})/2$, where \mathbf{B}^+ is the positive part of a matrix \mathbf{B} and \mathbf{B}^- is the negative part of a matrix \mathbf{B} . Note that for any $\mathbf{B}_{i,j}$, we have $\mathbf{B}_{i,j}^+ > 0$ and $\mathbf{B}_{i,j}^- \leq 0$. Thus, the separate can ensure the square root in Eq. (3) is meaningful. In addition, $\mathbf{B}_{i,j}^+ + \mathbf{B}_{i,j}^- = |\mathbf{B}_{i,j}|$ and $\mathbf{B}_{i,j}^+ - \mathbf{B}_{i,j}^- = \mathbf{B}_{i,j}$.

C. Extending to Semi-RNMF

In real-word applications, we often predict clusters by RMF and extract the latent feature information by semi-NMF. To improve the clustering performance, a natural idea is to combine RMF and semi-NMF, so we propose the semi-RNMF framework as follows:

$$\begin{aligned} & \min_{\mathbf{U}, \mathbf{V}} \|\mathbf{X} - \mathbf{UV}^T\|_F^2 + \alpha(\|\mathbf{U}\|_F^2 + \|\mathbf{V}\|_F^2) \\ & \text{s.t. } \mathbf{V}_{i,j} \geq 0, i \in [n], j \in [k]. \end{aligned} \quad (4)$$

We can update \mathbf{U} (while fixing \mathbf{V}) by $\mathbf{U} = \mathbf{XV}(\alpha\mathbf{I} + \mathbf{V}^T\mathbf{V})^{-1}$.

Based on the Karush-Kuhn-Tucker (KKT) complementarity condition for the nonnegativity of \mathbf{V} , we can update \mathbf{V} (while fixing \mathbf{U}) by

$$\mathbf{V}_{i,j} = \mathbf{V}_{i,j} \cdot \sqrt{\frac{(\mathbf{X}^T\mathbf{U})_{i,j}^+ + [\mathbf{V}(\alpha\mathbf{I} + \mathbf{U}^T\mathbf{U})]_{i,j}^-}{(\mathbf{X}^T\mathbf{U})_{i,j}^- + [\mathbf{V}(\alpha\mathbf{I} + \mathbf{U}^T\mathbf{U})]_{i,j}^+}}. \quad (5)$$

D. Extending to Incomplete Multi-view Clustering

To solve the incomplete multi-view clustering problem, we need to extend Eq. (4). For an incomplete multi-view dataset $\{\mathbf{X}^{(v)}\}_{v=1}^m$, we assume that different views have distinct basis matrices $\{\mathbf{U}^{(v)}\}_{v=1}^m$ and a common latent feature matrix \mathbf{V} .

First, we define an n -dimensional column vector $\mathbf{g}^{(v)}$ to indicate the incompleteness:

$$\mathbf{g}_i^{(v)} = \begin{cases} 1, & \text{if the } i\text{-th instance is in the } v\text{-th view;} \\ 0, & \text{otherwise.} \end{cases} \quad (6)$$

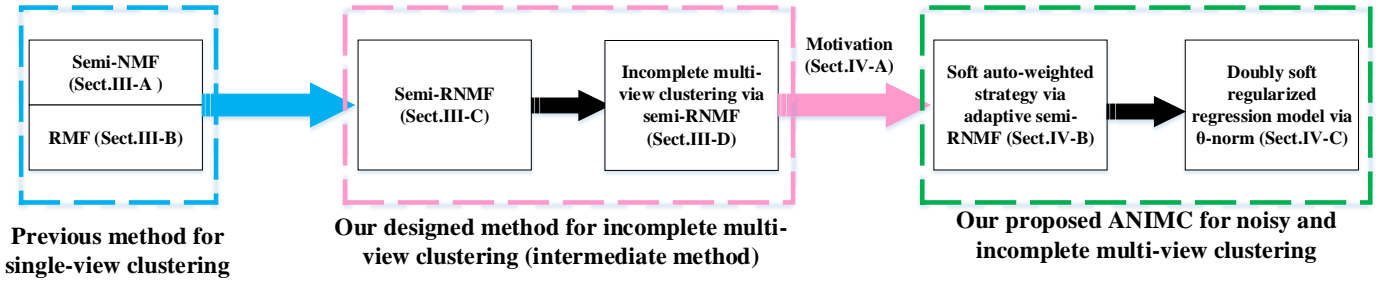


Fig. 1: The structure of the paper. ‘‘Sect.’’ denotes ‘‘Section’’.

To facilitate matrix operations, we extend $\mathbf{g}^{(v)}$ into an incomplete indicator matrix $\mathbf{G}^{(v)} \in \mathbb{R}^{d_v \times n}$:

$$\mathbf{G}_{:,i}^{(v)} = \begin{cases} 1, & \text{if the } i\text{-th instance is in the } v\text{-th view;} \\ 0, & \text{otherwise,} \end{cases} \quad (7)$$

where $\mathbf{G}_{:,i}^{(v)} = 1$ denotes that the elements in the i -th column of matrix $\mathbf{G}^{(v)}$ are all 1. Note that when the v -th view contains all the instances, the matrix $\mathbf{G}^{(v)}$ is an all-one matrix. If the v -th view miss some instances, the view matrix $\mathbf{X}^{(v)}$ will miss the corresponding columns, and the corresponding columns in $\mathbf{G}^{(v)}$ will become 0, i.e., $\sum_{i=1}^n \mathbf{G}_{t,i}^{(v)} < n$ (where $t \in [d_v]$).

Second, we extend Eq. (4) to

$$\begin{aligned} \min_{\mathbf{U}^{(v)}, \mathbf{V}} \sum_v (\|\mathbf{G}^{(v)} \odot (\mathbf{X}^{(v)} - \mathbf{U}^{(v)} \mathbf{V}^T)\|_F^2 \\ + \alpha (\|\mathbf{U}^{(v)}\|_F^2 + \|\mathbf{V}\|_F^2)) \\ \text{s.t. } \mathbf{V}_{i,j} \geq 0, i \in [n], j \in [k], \end{aligned} \quad (8)$$

where $\mathbf{U}^{(v)} \in \mathbb{R}^{d_v \times c}$, $\mathbf{V} \in \mathbb{R}^{n \times c}$, and \odot is the operation that multiplies two matrices by multiplying corresponding elements. But this extension is not satisfactory, we will propose a better method in the next section.

IV. PROPOSED ANIMC APPROACH

By showing the drawback of the direct extension to incomplete multi-view clustering, we first present the motivation of our proposed Auto-weighted Noisy and Incomplete Multi-view Clustering (ANIMC) approach. Then we model ANIMC as the joint of a soft auto-weighted strategy and a doubly soft regularized regression model.

A. Motivation

Note that Eq. (8) is the root function to integrate different incomplete views. For different tasks, we may need different functions with stronger generalization ability than Eq. (8). A feasible idea is extending Eq. (8) to a series of exponential functions. Thus, we can rewrite Eq. (8) as

$$\begin{aligned} \min_{\mathbf{U}^{(v)}, \mathbf{V}} \sum_v (\|\mathbf{G}^{(v)} \odot (\mathbf{X}^{(v)} - \mathbf{U}^{(v)} \mathbf{V}^T)\|_F^r \\ + \alpha (\|\mathbf{U}^{(v)}\|_F^2 + \|\mathbf{V}\|_F^2)) \\ \text{s.t. } \mathbf{V}_{i,j} \geq 0, i \in [n], j \in [k], \end{aligned} \quad (9)$$

where $0 < r \leq 2$. As r changes, we can obtain different exponential functions. By choosing different exponential functions, Eq. (9) can integrate all views on different tasks.

However, Eq. (9) cannot distinguish the availability of different views because Eq. (9) does not define the weight factor (i.e., importance) for each view. Intuitively, Eq. (9) only simply fills the missing instances into each view, which cannot effectively leverage the consistent information between views. If we use $\mathbf{E}^{(v)} = \mathbf{X}^{(v)} - \mathbf{U}^{(v)} \mathbf{V}^T$ to represent the noises, and $(\mathbf{G}^{(v)} \odot \mathbf{E}^{(v)})$ can represent the combination of noises and incompleteness. For a noisy and incomplete multi-view dataset, we assume that a view with more noises will have a larger $\mathbf{E}^{(v)}$. Eq. (9) is difficult to deal with noises effectively because these noisy views have a greater impact on the objective function. What is worse, Eq. (9) pushes the noisy view with the lowest clustering availability hardest, which hurts the clustering performance. Therefore, we need a soft auto-weighted model to adaptively weight each view.

B. Soft Auto-weighted Strategy Via Adaptive Semi-RNMF

Different views have distinct availability, but the common latent feature matrix \mathbf{V} does not directly contain the information about the availability of each view. The information can distinguish different views and will also affect clustering results. Therefore, a clever way is to obtain the optimal \mathbf{V} and distinguish the availability of different views simultaneously through one iteration. Although Eq. (9) can integrate multiple views, it is difficult to distinguish the availability of different views after obtaining \mathbf{V} . It is because Eq. (9) does not assign weights to these views.

Therefore, we propose a novel model named adaptive semi-RNMF to assign a proper weight to each view and learn optimal \mathbf{V} , simultaneously. It relies on the following two intuitive assumptions for a noisy and incomplete multi-view dataset $\{\mathbf{X}^{(v)}\}_{v=1}^m$: (i) $\mathbf{X}^{(v)}$ is the perturbation of $\mathbf{U}^{(v)} \mathbf{V}^T$ due to noises; and (ii) incomplete views with more noises should have smaller weights. To learn optimal latent feature matrix \mathbf{V} , we can design the Lagrangian function as follows:

$$\sum_v \|\mathbf{G}^{(v)} \odot (\mathbf{X}^{(v)} - \mathbf{U}^{(v)} \mathbf{V}^T)\|_F^r + \alpha \|\mathbf{V}\|_F^2 + \zeta(\Lambda, \mathbf{V}), \quad (10)$$

where Λ is the Lagrange multiplier and $\zeta(\Lambda, \mathbf{V})$ is a proxy for the constraints. Setting the derivative of Eq. (10) w.r.t. \mathbf{V} to zero, we can obtain

$$\begin{aligned} \sum_v w_v \frac{\partial \|\mathbf{G}^{(v)} \odot (\mathbf{X}^{(v)} - \mathbf{U}^{(v)} \mathbf{V}^T)\|_F^r}{\partial \mathbf{V}} + \frac{\partial \alpha \|\mathbf{V}\|_F^2}{\partial \mathbf{V}} \\ + \frac{\partial \zeta(\Lambda, \mathbf{V})}{\partial \mathbf{V}} = \mathbf{0}, \end{aligned} \quad (11)$$

where

$$w_v = 0.5r \|\mathbf{G}^{(v)} \odot (\mathbf{X}^{(v)} - \mathbf{U}^{(v)} \mathbf{V}^T)\|_F^{0.5r-1}. \quad (12)$$

In Eq. (12), w_v depends on the target variable \mathbf{V} , so we cannot directly obtain w_v . To solve Eq. (12), we first set w_v fixed and update w_v after obtaining $\mathbf{U}^{(v)}$ and \mathbf{V} . If we fix w_v , Eq. (11) can be viewed as the solution to the following problem:

$$\begin{aligned} \min_{w_v, \mathbf{U}^{(v)}, \mathbf{V}} \sum_v (w_v \|\mathbf{G}^{(v)} \odot (\mathbf{X}^{(v)} - \mathbf{U}^{(v)} \mathbf{V}^T)\|_F^2 \\ + \alpha (\|\mathbf{U}^{(v)}\|_F^2 + \|\mathbf{V}\|_F^2)) \\ w_v = 0.5r \|\mathbf{G}^{(v)} \odot (\mathbf{X}^{(v)} - \mathbf{U}^{(v)} \mathbf{V}^T)\|_F^{0.5r-1}. \end{aligned} \quad (13)$$

But there is a case that fails Eq. (13). As the missing rate grows, the zero elements of $\mathbf{G}^{(v)}$ in Eq. (13) will also increase, and the view weight will enlarge. However, too-large weights will focus too much on the incompleteness and ignore the noises, which is difficult to reflect the impact of noises on clustering. Therefore, we need to add a soft boundary to w_v :

$$\begin{aligned} w_v = \min(0.5r \|\mathbf{G}^{(v)} \odot (\mathbf{X}^{(v)} - \mathbf{U}^{(v)} \mathbf{V}^T)\|_F^{0.5r-1}, \\ \|\mathbf{X}^{(v)} - \mathbf{U}^{(v)} \mathbf{V}^T\|_F^{-0.5}), \end{aligned} \quad (14)$$

where $0.5 \|\mathbf{X}^{(v)} - \mathbf{U}^{(v)} \mathbf{V}^T\|_F^{-0.5}$ is the boundary value of Eq. (12), which is a special case that the dataset is a complete multi-view dataset with $r = 1$. Based on function $\min(\cdot)$, $\|\mathbf{X}^{(v)} - \mathbf{U}^{(v)} \mathbf{V}^T\|_F^{-0.5}$ can reflect the effect of noises on clustering when the missing rate is relatively large. Therefore, the final model of adaptive semi-RNMF is

$$\begin{aligned} \min_{w_v, \mathbf{U}^{(v)}, \mathbf{V}} \sum_v (w_v \|\mathbf{G}^{(v)} \odot (\mathbf{X}^{(v)} - \mathbf{U}^{(v)} \mathbf{V}^T)\|_F^2 \\ + \alpha (\|\mathbf{U}^{(v)}\|_F^2 + \|\mathbf{V}\|_F^2)) \\ w_v = \min(0.5r \|\mathbf{G}^{(v)} \odot (\mathbf{X}^{(v)} - \mathbf{U}^{(v)} \mathbf{V}^T)\|_F^{0.5r-1}, \\ \|\mathbf{X}^{(v)} - \mathbf{U}^{(v)} \mathbf{V}^T\|_F^{-0.5}) \\ \text{s.t. } \mathbf{V}_{ij} \geq 0, i \in [n], j \in [k]. \end{aligned} \quad (15)$$

Note that Eq. (15) is a soft model and we can learn different weight functions $\{w_v\}_{v=1}^m$ by changing r , which enhances its generalization ability. After fixing w_v , the Lagrangian function Eq. (10) also applies to Eq. (15). After we obtain \mathbf{V} from Eq. (15), we can update w_v , which inspires us to optimize Eq. (9) by an alternative method. After optimization, the updated \mathbf{V} is at least locally optimal. For the v -th view, $\mathbf{G}^{(v)}$ indicates the missing rate and perturbation $(\mathbf{X}^{(v)} - \mathbf{U}^{(v)} \mathbf{V}^T)$ represents noises. Through the above two aspects, w_v can effectively distinguish different views, which meets our intuitive assumptions about weight. Also, Eq. (15) updates both the optimal \mathbf{V} and w_v simultaneously. Moreover, Eq. (15) not only learns the optimal \mathbf{V} , but also distinguishes different views automatically. Besides, w_v considers the combined effects of noises and incompleteness. Therefore, we regard w_v as the weight of the v -th view.

C. Doubly Soft Regularized Regression Model via θ -norm

Note that $\alpha (\|\mathbf{U}^{(v)}\|_F^2 + \|\mathbf{V}\|_F^2)$ (in Eq. (15)) serves as the regular term of $\mathbf{U}^{(v)}$ and \mathbf{V} . As for $w_v \|\mathbf{G}^{(v)} \odot (\mathbf{X}^{(v)} - \mathbf{U}^{(v)} \mathbf{V}^T)\|_F^2$ (in Eq. (15)), it is used to fill missing instances

into the view matrix. In most cases, the filling strategy is difficult to achieve good results because it cannot effectively use the information of the presented instances to complete the view matrix. In the field of statistics, regularized regression is an efficient tool for matrix completion on real-world incomplete data. To decrease the impact of missing instances, we try to design a doubly regularized regression model to cluster noisy and incomplete multi-view data. Based on the model, we attempt to push the latent feature matrix \mathbf{V} towards the consensus feature matrix (denoted by \mathbf{V}^*) and align basis matrices $\{\mathbf{U}^{(v)}\}_{v=1}^m$ to the consensus basis matrix (denoted by \mathbf{U}^*).

First, we design the F-norm regularized regression to push \mathbf{V} closer to \mathbf{V}^* . To reduce the disagreement between \mathbf{V} and \mathbf{V}^* , we leverage the F-norm, which corresponds to Euclidean distance. Thus, we have

$$\min_{\mathbf{V}} (\|\mathbf{V} - \mathbf{V}^*\|_F^2 + \eta \|\mathbf{V}\|_F^2), \quad (16)$$

where η is a nonnegative parameter.

Second, to align the basis matrices $\mathbf{U}^{(v)}$ of the same instance in different views, we adopt the following regularized regression function based on the F-norm:

$$\min_{\mathbf{U}^{(v)}, \mathbf{A}^{(v)}} \sum_v (\|\mathbf{A}^{(v)T} \mathbf{U}^{(v)} - \mathbf{U}^*\|_F^2 + \beta \|\mathbf{A}^{(v)}\|_F^2), \quad (17)$$

where $\mathbf{A}^{(v)} \in \mathbb{R}^{d_v \times c}$ is the regression coefficient matrix of the v -th view and β is a nonnegative parameter.

For a particular incomplete dataset, its $\mathbf{V}^* \in \mathbb{R}^{n \times c}$ and $\mathbf{U}^* \in \mathbb{R}^{c \times c}$ are constant. In general, they are low-rank for all the views, and the cluster number c plays an important role in clustering. For most tasks, we need not obtain specific \mathbf{V}^* and \mathbf{U}^* , and we will get satisfactory clustering results by learning correct c . Therefore, we can find simple matrices as substitutes for \mathbf{V}^* and \mathbf{U}^* to simplify Eq. (16) and Eq. (17):

(i) Substitute for \mathbf{V}^* : since all the views share the same \mathbf{V} , \mathbf{V} contains the consistent information of all views. The available consistent information is the guarantee of satisfactory clustering results. For different clustering tasks (e.g., different datasets, different missing rates, or different noise rates), we often have different \mathbf{V}^* . For matrix \mathbf{V} , we assume that due to the influence of noises we have $0 < \mathbf{V}_{i,j}^* < \mathbf{V}_{i,j}$.

For example, for a noisy and incomplete multi-view dataset, under different cases (different noises or different incompleteness), we will get different \mathbf{V}^* . To ensure that we can obtain a suitable regularized regression model in different situations, we need to ensure that the regularized regression model is suitable for different cases. To improve the generalization ability of Eq. (16) (i.e., for different \mathbf{V}^* , we can obtain satisfactory clustering results), we should simplify Eq. (16) reasonably. For any matrix \mathbf{V}^* ($0 < \mathbf{V}_{i,j}^* < \mathbf{V}_{i,j}$), we have $\lim_{\mathbf{V}_{i,j}^* \rightarrow 0^+} \|\mathbf{V} - \mathbf{V}^*\|_F = \|\mathbf{V}\|_F$. When $\mathbf{V}^* \rightarrow \mathbf{V}$, we have $(\|\mathbf{V} - \mathbf{V}^*\|_F^2 + \eta \|\mathbf{V}\|_F^2) \rightarrow \eta \|\mathbf{V}\|_F^2$; when $\mathbf{V}^* \rightarrow \mathbf{0}$, we have $(\|\mathbf{V} - \mathbf{V}^*\|_F^2 + \eta \|\mathbf{V}\|_F^2) \rightarrow (1 + \eta) \|\mathbf{V}\|_F^2$. Note that $\eta \|\mathbf{V}\|_F^2 < (\|\mathbf{V} - \mathbf{V}^*\|_F^2 + \eta \|\mathbf{V}\|_F^2) < (1 + \eta) \|\mathbf{V}\|_F^2$. Thus, $(\|\mathbf{V} - \mathbf{V}^*\|_F^2 + \eta \|\mathbf{V}\|_F^2) < (1 + \eta) \|\mathbf{V}\|_F^2$ in all the cases. Obviously, $(1 + \eta) \|\mathbf{V}\|_F^2$ is the upper limit of $(\|\mathbf{V} - \mathbf{V}^*\|_F^2 + \eta \|\mathbf{V}\|_F^2)$. When we minimize $(\|\mathbf{V} - \mathbf{V}^*\|_F^2 + \eta \|\mathbf{V}\|_F^2)$, we

only need to minimize its upper limit to ensure the availability of our method in different datasets with different \mathbf{V}^* , which illustrates the generalization ability of our algorithm. Therefore, we can shrink Eq. (16) to

$$\min_{\mathbf{V}} (1 + \eta) \|\mathbf{V}\|_F^2. \quad (18)$$

Since η is nonnegative, we can transform Eq. (18) into

$$\min_{\mathbf{V}} \|\mathbf{V}\|_F^2. \quad (19)$$

(ii) Substitute for \mathbf{U}^* : for most real-world applications, we need to integrate the consistent information of different views for clustering. Fortunately, we can maximize the consistent information by pushing the latent feature matrix towards the consensus feature matrix. When performing the regularized regression on \mathbf{U}^* , we only need to cluster n instances into c clusters. Thus, we prefer to obtain an effective c rather than a specific \mathbf{U}^* . Since \mathbf{U}^* is a c dimensional square matrix, we can leverage a c -dimensional identity matrix \mathbf{I} as an alternative to \mathbf{U}^{*2} . Therefore, we can rewrite Eq. (17) as

$$\min_{\mathbf{U}^{(v)}, \mathbf{A}^{(v)}} \sum_v (\|\mathbf{A}^{(v)T} \mathbf{U}^{(v)} - \mathbf{I}\|_F^2 + \beta \|\mathbf{A}^{(v)}\|_F^2). \quad (20)$$

However, the regularized regression based on F-norm is difficult to learn the sparse $\mathbf{U}^{(v)}$ and \mathbf{V} for clustering. Because F-norm cannot select features across all data points with joint sparsity. To obtain a more robust regularized regression model, we design a doubly soft regularized regression model by designing a novel θ -norm.

For any matrix \mathbf{B} , its F-norm is defined as

$$\|\mathbf{B}\|_F = \sqrt{\sum_i \sum_j \mathbf{B}_{i,j}^2}. \quad (21)$$

Inspired by Eq. (21), we define the θ -norm of matrix \mathbf{B} as

$$\|\mathbf{B}\|_\theta = \sum_i \frac{(1 + \theta)(\sum_j \mathbf{B}_{i,j}^2)^2}{1 + \theta \sum_j \mathbf{B}_{i,j}^2}, \quad (22)$$

where we can choose the proper θ according to our needs. Based on matrix \mathbf{B} , we design a diagonal matrix \mathbf{D}_B defined as

$$\mathbf{D}_{B_{i,i}} = \frac{2 + \theta(\sum_j \mathbf{B}_{i,j}^2 + 2) + \theta^2 \sum_j \mathbf{B}_{i,j}^2}{\theta^2(\sum_j \mathbf{B}_{i,j}^2)^2 + 2\theta \sum_j \mathbf{B}_{i,j}^2 + 1}. \quad (23)$$

Theorem 1. For any $\theta > 0$, we have

$$\frac{\partial \|\mathbf{B}\|_\theta}{\partial \mathbf{B}} = \mathbf{D}_B \mathbf{B}. \quad (24)$$

Proof:

$$\begin{aligned} \frac{\partial \|\mathbf{B}\|_\theta}{\partial \mathbf{B}_{i,:}} &= \frac{\partial((1 + \theta)\|\mathbf{B}_{i,:}\|_2^2 / (1 + \theta\|\mathbf{B}_{i,:}\|_2))}{\partial \mathbf{B}_{i,:}} \\ &= \frac{2 + \theta(\|\mathbf{B}_{i,:}\|_2 + 2) + \theta^2 \|\mathbf{B}_{i,:}\|_2}{\theta^2 \|\mathbf{B}_{i,:}\|_2^2 + 2\theta \|\mathbf{B}_{i,:}\|_2 + 1} \mathbf{B}_i = \mathbf{D}_{B_{i,i}} \mathbf{B}_{i,:}. \end{aligned} \quad (25)$$

Our proposed θ -norm has the following characteristics:

1) θ -norm is nonnegative and global differentiable;

²The forms of different alternatives have little effect on the clustering performance and we choose \mathbf{I} as the alternative for simplicity.

2) when $\theta \rightarrow \infty$, we have $\|\mathbf{B}\|_\theta \rightarrow \|\mathbf{B}\|_{2,1}$ and $\mathbf{D}_{B_{i,i}} \rightarrow 1/\|\mathbf{B}_{i,:}\|_2$;

3) when $\theta \rightarrow 0$, we have $\|\mathbf{B}\|_\theta \rightarrow \|\mathbf{B}\|_F^2$ and $\mathbf{D}_B \rightarrow \mathbf{I}$.

As θ increases, $\|\mathbf{B}\|_\theta$ is closer to $\|\mathbf{B}\|_{2,1}$ and \mathbf{B} becomes more sparse. Since we can choose different θ to adjust the sparsity of the matrix, θ -norm can be viewed as a soft norm with a strong generalization ability. Besides, the global differentiability of θ -norm can ensure that we can learn the correct derivative, which is significant for the following optimization (see Section IV-E). Therefore, we transform Eq. (19) into

$$\min_{\mathbf{V}} \|\mathbf{V}\|_\theta. \quad (26)$$

Similarly, we transform Eq. (20) into

$$\min_{\mathbf{U}^{(v)}, \mathbf{A}^{(v)}} \sum_v (\|\mathbf{A}^{(v)T} \mathbf{U}^{(v)} - \mathbf{I}\|_F^2 + \beta \|\mathbf{A}^{(v)}\|_\theta). \quad (27)$$

Combining Eq. (26) and Eq. (27), we can obtain the doubly soft regularized regression model as follows

$$\min_{\mathbf{U}^{(v)}, \mathbf{V}, \mathbf{A}^{(v)}} \sum_v (\|\mathbf{A}^{(v)T} \mathbf{U}^{(v)} - \mathbf{I}\|_F^2 + \beta \|\mathbf{A}^{(v)}\|_\theta) + \|\mathbf{V}\|_\theta. \quad (28)$$

For the soft model Eq. (28), we can change its sparsity by adjusting θ , which improves its generalization ability.

D. Objective Function

Considering the objective for soft auto-weighted strategy (Eq. (15)) and doubly soft regularized regression model (Eq. (28)), we minimize the following problem:

$$\begin{aligned} L &= \sum_v (w_v \|\mathbf{G}^{(v)} \odot (\mathbf{X}^{(v)} - \mathbf{U}^{(v)} \mathbf{V}^T)\|_F^2 \\ &\quad + \alpha \|\mathbf{A}^{(v)T} \mathbf{U}^{(v)} - \mathbf{I}\|_F^2 + \beta \|\mathbf{A}^{(v)}\|_\theta) + \alpha \|\mathbf{V}\|_\theta \\ w_v &= \min(0.5r \|\mathbf{G}^{(v)} \odot (\mathbf{X}^{(v)} - \mathbf{U}^{(v)} \mathbf{V}^T)\|_F^{0.5r-1}, \\ &\quad \|\mathbf{X}^{(v)} - \mathbf{U}^{(v)} \mathbf{V}^T\|_F^{-0.5}) \\ \text{s.t. } &\mathbf{V}_{i,j} \geq 0, i \in [n], j \in [k], \end{aligned} \quad (29)$$

where α and β are nonnegative parameters. Next, our experiments will show its effectiveness and efficiency of Eq. (29).

E. Optimization

Since Eq. (29) is not convex for all the variables simultaneously, inspired by Augmented Lagrange Multiplier (ALM) method [113], we design a four-step alternating iteration procedure to optimize it:

Step 1. Updating $\mathbf{U}^{(v)}$. Fixing the other variables, we need to minimize the following problem:

$$\begin{aligned} L(\mathbf{U}^{(v)}) &= w_v \|\mathbf{G}^{(v)} \odot (\mathbf{X}^{(v)} - \mathbf{U}^{(v)} \mathbf{V}^T)\|_F^2 \\ &\quad + \alpha \|\mathbf{A}^{(v)T} \mathbf{U}^{(v)} - \mathbf{I}\|_F^2. \end{aligned} \quad (30)$$

We can obtain $\mathbf{U}^{(v)}$ by setting the derivative of $L(\mathbf{U}^{(v)})$ w.r.t. $\mathbf{U}^{(v)}$ to zero as follows:

$$\begin{aligned} \frac{\partial L(\mathbf{U}^{(v)})}{\partial \mathbf{U}^{(v)}} &= 2w_v \mathbf{G}^{(v)} \odot (\mathbf{X}^{(v)} - \mathbf{U}^{(v)} \mathbf{V}^T) \mathbf{V} \\ &\quad + 2\alpha \mathbf{A}^{(v)} (\mathbf{A}^{(v)T} \mathbf{U}^{(v)} - \mathbf{I}) = \mathbf{0}. \end{aligned} \quad (31)$$

Algorithm 1 ANIMC

Input: Data matrices for noisy and incomplete views $\{\mathbf{X}^{(v)}\}_{v=1}^m \in \mathbb{R}^{d_v \times n}$, indicator matrix $\{\mathbf{G}^{(v)}\}_{v=1}^m \in \mathbb{R}^{d_v \times n}$, parameters $\{\alpha, \beta\}$, cluster number c .
 Choose parameters $\{\theta, r\}$ according to needs.
 Initialize regression coefficient matrix $\mathbf{A}^{(v)}$, basis matrix $\mathbf{U}^{(v)}$, view weight $w_v = 1/m$ for each view.
 Initialize common latent feature matrix \mathbf{V} .
 Initialize iteration time $i = 0$, maximum iteration time i_{\max} .
while Eq. (29) does not converge && $i \leq i_{\max}$ **do**
 Update $\mathbf{U}^{(v)}$ by Eq. (31);
 Update $\mathbf{A}^{(v)}$ by Eq. (38);
 Update \mathbf{V} by Eq. (42);
 Update w_v by Eq. (14);
 $i = i + 1$;
end while
Output: $\{\mathbf{A}^{(v)}\}_{v=1}^m$, $\{\mathbf{U}^{(v)}\}_{v=1}^m$, $\{w_v\}_{v=1}^m$, \mathbf{V} and clustering results.

The Eq. (31) is the Sylvester equation w.r.t. $\mathbf{U}^{(v)}$ [114]. Based on d_v and c , we can divide Eq. (31) into two cases to facilitate the solution.

Theorem 2. For the v -th view, denote $\mathbf{E}^{(v)} = \mathbf{X}^{(v)} - \mathbf{U}^{(v)}\mathbf{V}^T$, and we have $\mathbf{G}^{(v)} \odot \mathbf{E}^{(v)} = \mathbf{E}^{(v)}\mathbf{T}^{(v)}$.

Proof: For $\mathbf{G}^{(v)} \odot \mathbf{E}^{(v)}$, we have

$$(\mathbf{G}^{(v)} \odot \mathbf{E}^{(v)})_{i,j} = \begin{cases} \mathbf{E}_{i,j}^{(v)}, & \text{if instance } j \text{ is in view } v; \\ 0, & \text{otherwise.} \end{cases} \quad (32)$$

For $\mathbf{E}^{(v)}\mathbf{T}^{(v)}$, we have

$$(\mathbf{E}^{(v)}\mathbf{T}^{(v)})_{i,j} = \begin{cases} \mathbf{E}_{i,j}^{(v)}, & \text{if instance } j \text{ is not in view } v; \\ 0, & \text{otherwise.} \end{cases} \quad (33)$$

Note that $\mathbf{G}^{(v)} \odot \mathbf{E}^{(v)}$ and $\mathbf{E}^{(v)}\mathbf{T}^{(v)}$ have the same size. Besides, $(\mathbf{G}^{(v)} \odot \mathbf{E}^{(v)})_{i,j} = (\mathbf{E}^{(v)}\mathbf{T}^{(v)})_{i,j}$ in all cases, which proves Theorem 2. ■

(i) When both d_v and c are small, based on Theorem 2, we can update $\mathbf{U}^{(v)}$ by

$$\text{vec}(\mathbf{U}^{(v)}) = [\mathbf{I} \otimes ((w_v \mathbf{V}^T \mathbf{T}^{(v)} \mathbf{V}) \otimes \mathbf{I} + \alpha \mathbf{A}^{(v)} \mathbf{A}^{(v)T})^{-1} \text{vec}(\alpha \mathbf{A}^{(v)} + w_v \mathbf{X}^{(v)} \mathbf{T}^{(v)} \mathbf{V})], \quad (34)$$

where $\text{vec}(\cdot)$ is the vectorization operation; \otimes is the Kronecker product; $\mathbf{T}^{(v)} \in \mathbb{R}^{n \times n}$ is the corresponding diagonal matrix of vector $\mathbf{g}^{(v)}$.

(ii) When both d_v and c are large, the solution is solved by a conjugate gradient [115]. For ease of calculation, Eq. (31) can be approximated as the Lyapunov equation [116].

Step 2. Updating $\mathbf{A}^{(v)}$. Fixing the other variables, we need to minimize the following problem:

$$L(\mathbf{A}^{(v)}) = \alpha \|\mathbf{A}^{(v)T} \mathbf{U}^{(v)} - \mathbf{I}\|_F^2 + \beta \|\mathbf{A}^{(v)}\|_\theta. \quad (35)$$

We can obtain $\mathbf{A}^{(v)}$ by setting the derivative of $L(\mathbf{A}^{(v)})$ w.r.t. $\mathbf{A}^{(v)}$ to zero as follows:

$$\alpha \mathbf{U}^{(v)} \mathbf{U}^{(v)T} \mathbf{A}^{(v)} - \mathbf{U}^{(v)} + \beta \mathbf{D}_A^{(v)} \mathbf{A}^{(v)} = \mathbf{0}. \quad (36)$$

By solving Eq. (36), $\mathbf{A}^{(v)}$ can be updated by

$$\mathbf{A}^{(v)} = [\alpha \mathbf{U}^{(v)} \mathbf{U}^{(v)T} + \beta \mathbf{D}_A^{(v)}]^{-1} \mathbf{U}^{(v)}. \quad (37)$$

In most image processing applications, $\mathbf{U}^{(v)}$ has a large number of rows and a small number of columns and $(\mathbf{U}^{(v)} \mathbf{U}^{(v)T} + \beta \mathbf{D}_A^{(v)})$ is close to singular, so we can use the Woodbury matrix identity [117] to simplify the calculation. Thus, we have

$$\mathbf{A}^{(v)} = \frac{\alpha}{\beta} [\mathbf{D}_A^{(v)-1} - \mathbf{D}_A^{(v)-1} \mathbf{U}^{(v)} (\mathbf{U}^{(v)T} \mathbf{D}_A^{(v)-1} \mathbf{U}^{(v)} + \beta \mathbf{I})^{-1} \mathbf{U}^{(v)T} \mathbf{D}_A^{(v)-1}] \mathbf{U}^{(v)}. \quad (38)$$

Step 3. Updating \mathbf{V} . Fixing the other variables, we need to minimize the following problem:

$$L(\mathbf{V}) = \sum_v w_v \|\mathbf{G}^{(v)} \odot (\mathbf{X}^{(v)} - \mathbf{U}^{(v)} \mathbf{V}^T)\|_F^2 + \alpha \|\mathbf{V}\|_\theta. \quad (39)$$

We can obtain \mathbf{V} by setting the derivative of $L(\mathbf{V})$ w.r.t. \mathbf{V} to zero as follows:

$$\sum_v w_v ((\mathbf{G}^{(v)} \odot \mathbf{U}^{(v)} \mathbf{V}^T)^T - (\mathbf{G}^{(v)} \odot \mathbf{X}^{(v)})^T) \mathbf{U}^{(v)} + \beta \mathbf{D}_V \mathbf{V} = \mathbf{0}. \quad (40)$$

Similar to [107], based on the KKT complementarity condition for the nonnegativity of \mathbf{V} , we have

$$\left(\sum_v w_v ((\mathbf{G}^{(v)} \odot \mathbf{U}^{(v)} \mathbf{V}^T)^T - (\mathbf{G}^{(v)} \odot \mathbf{X}^{(v)})^T) \mathbf{U}^{(v)} + \beta \mathbf{D}_V \mathbf{V} \right)_{i,j} \mathbf{V}_{i,j} = 0. \quad (41)$$

Therefore, \mathbf{V} can be updated by

$$\mathbf{V}_{i,j} \leftarrow \mathbf{V}_{i,j} \cdot \sqrt{\frac{[\mathbf{Z}_1]_{i,j}^+ + [\mathbf{Z}_2]_{i,j}^-}{[\mathbf{Z}_1]_{i,j}^- + [\mathbf{Z}_2]_{i,j}^+}}, \quad (42)$$

where $\mathbf{Z}_1 = \sum_v w_v (\mathbf{G}^{(v)} \odot \mathbf{X}^{(v)})^T \mathbf{U}^{(v)}$ and $\mathbf{Z}_2 = \sum_v w_v (\mathbf{G}^{(v)} \odot \mathbf{U}^{(v)} \mathbf{V}^T)^T \mathbf{U}^{(v)} + \alpha \mathbf{D}_V \mathbf{V}$.

In Step 1 and Step 3, we often need to normalize $\mathbf{U}^{(v)}$ and \mathbf{V} to ensure the accuracy of the updating rules [93], so $\mathbf{U}^{(v)}$ and \mathbf{V} can be normalized by $\mathbf{U}^{(v)} \leftarrow \mathbf{U}^{(v)} \mathbf{Q}$, $\mathbf{V} \leftarrow \mathbf{V} \mathbf{Q}^{-1}$, where \mathbf{Q} is the diagonal matrix $\mathbf{Q}_{k,k}^{(v)} = \sum_t \mathbf{V}_{t,k}$.

Step 4. Updating w_v . Fixing the other variables, we can update the variable w_v by Eq. (14).

Our proposed ANIMC algorithm is shown in Algorithm 1. We provide its codes in GitHub (https://github.com/ZeusDavide/TAI_2021_ANIMC).

F. Convergence and Complexity

1) *Convergence Analysis:* To optimize our proposed ANIMC, we need to solve four subproblems in Algorithm 1. Each subproblem is convex and has the closed solution w.r.t corresponding variable. Thus, the objective function Eq. (29) will reduce monotonically to a stationary point, which ensures that ANIMC can at least find a locally optimal solution.

2) *Complexity Analysis*: As shown in Algorithm 1, the operations of updating four parameters ($\mathbf{U}^{(v)}$, $\mathbf{A}^{(v)}$, \mathbf{V} , and w_v) determine the computational complexity of the algorithm. Assume i is the number of iterations, the time complexities of updating $\mathbf{U}^{(v)}$, $\mathbf{A}^{(v)}$, \mathbf{V} and w_v are respectively $O(d_v^2 c + n(d_v + c))$, $O(c(d_v^2 + c^2))$, $O(ic(nd_v + cd_v + nc))$ and $O(nc^2)$. Since $c \ll \min(d_v, n)$ in most image processing applications, the total complexity is $O(\max(d_v, n)(ci + d_v^2))$.

V. PERFORMANCE EVALUATION

A. Datasets

TABLE I: Statistics of the datasets

Dataset	#. instances	#. views	#. clusters	#. features
BBCSport	544	2	5	6386
BUAA	180	2	20	200
Caltech7	1474	6	7	3766
Digit	2000	5	10	585
NH-face	4660	5	5	12054
Scene	2688	4	8	1248

To evaluate the effectiveness of our proposed ANIMC approach in real-world tasks, we conduct experiments on six real-world multi-view datasets as follows: BBCSport³ [118], BUAA [119], Digit⁴, Scene [120], Caltech7 [121], and NH_face [122], whose statistics are summarized in Table I.

Most multi-view clustering algorithms often cluster their subsets for simplicity. To compare fairly with these algorithms, we use the same subsets for clustering. The detailed information of used datasets is as follows:

BBCSport: The original BBCSport dataset contains 737 documents (instances), which are described by 2-4 views and categorized into 5 clusters. Following [95], we choose a subset with 544 instances and 2 views.

BUAA: The dataset is an image dataset, which is described by two views. Following [95], we use its subset with 180 instances and 10 clusters.

Caltech7: The dataset is a subset of the Caltech101 dataset. The dataset has 1474 instances consisting of 7 clusters. Each instance has 6 views.

Digit: It is a handwritten dataset. Following [93], we use its subset with 2000 instances, 10 clusters, and 5 views.

NH_face: It is a movie dataset, which contains 4660 faces from 5 persons. Each face has 3 views.

Scene: The dataset is an outdoor Scene dataset. Following [123], the dataset has 2688 images (instances) consisting of 8 clusters. Each image has 4 views.

B. Compared Methods

We compare our proposed ANIMC approach with eleven state-of-the-art methods:

1) **AGC_IMC** [124] develops a joint framework for graph completion and consensus representation learning.

2) **BSV** [102] first fills all missing instances in the average instance of each view, then implements K-means clustering

on every single view, separately. Finally, BSV reports the best performance.

3) **Concat** [102] first combines all views into a single view by concatenating their view matrices. Then, Concat implements K-means clustering on the single view and reports the clustering results.

4) **DAIMC** [94] extends MIC [93] by designing weighted semi-NMF and $L_{2,1}$ -norm regularized regression.

5) **EE-IMVC** [108] proposes a late fusion approach to simultaneously clustering and imputing the incomplete base clustering matrices.

6) **EE-R-IMVC** [109] improves EE-IMVC by incorporating prior knowledge to regularize the learned consensus clustering matrix.

7) **MIC** [93] extends PVC via weighted NMF and $L_{2,1}$ -norm regularization.

8) **MLAN** [96] is a self-weighted framework for complete multi-view clustering. By learning the optimal graph, it performs clustering and local structure learning simultaneously.

9) **NMF-CC** [88] aims to capture the intra-view diversity and learning many independent basis matrices in turn for a satisfactory clustering representation.

10) **UEAF** [95] learns a consensus representation for all views by extending MIC.

11) **UIMC** [64] is the first effective method to cluster multiple views with different incompleteness.

Since NMF-CC and MLAN cannot directly handle incomplete multi-view data, following [94], we fill the missing instances with average feature values. Note that our proposed ANIMC has two parameters (α and β), and we adjust them to obtain the best performance.

Following [101] and [102], we repeat each incomplete multi-view clustering experiment 10 times to obtain the average performance. Following [95], we randomly delete some instances from each view to make these views incomplete and set the missing rate (PER) from 0.1 to 0.5 (each view has 50% instances missing) with 0.2 as an interval.

Following [95], we evaluate the experimental results by three popular metrics: Accuracy (ACC), Normalized Mutual Information (NMI), and Purity. [88] provides the calculation method of these metrics. For these metrics, the larger value represents better clustering performance. All results of compared methods are produced by released codes, some of which may be inconsistent with published information due to different pretreatment processes. All the codes in the experiments are implemented in MATLAB R2019b and run on a Windows 10 machine with 3.30 GHz E3-1225 CPU, 64 GB main memory.

C. Incomplete Multi-view Clustering

Table II shows the ACC, NMI and Purity values on these real-world datasets with various PERs. As PER increases, the performance of each method often decreases. Obviously, our proposed ANIMC significantly performs better than other state-of-the-art methods in all cases, which verifies its effectiveness and strong generalization ability.

BBCSport: As shown in Table II, compared with the other methods, MLAN often becomes the first worst. For example,

³<http://mlg.ucd.ie/datasets/segment.html>.

⁴<http://archive.ics.uci.edu/ml/datasets.html>.

TABLE II: Incomplete multi-view clustering results on various datasets. **Bold** numbers denote the best results.

Dataset	Method	ACC (%)			NMI (%)			Purity (%)		
		PER=0.1	PER=0.3	PER=0.5	PER=0.1	PER=0.3	PER=0.5	PER=0.1	PER=0.3	PER=0.5
BBCSport	AGC_IMC	56.01	43.64	39.18	50.75	29.47	17.43	54.65	40.85	39.68
	BSV	53.19	42.19	30.86	47.71	35.86	23.75	63.64	52.74	47.02
	Concat	50.36	45.81	36.98	50.90	32.97	19.07	68.91	53.44	44.81
	DAIMC	40.42	37.81	33.17	23.17	14.08	11.63	41.16	36.11	32.91
	EE-IMVC	55.97	43.97	40.77	51.66	30.15	18.53	50.42	37.18	30.11
	EE-R-IMVC	50.12	40.03	34.64	50.65	31.50	19.64	51.96	38.69	29.76
	MIC	38.71	31.94	30.15	20.41	18.40	16.85	48.35	40.01	36.13
	MLAN	47.13	29.61	19.46	17.42	5.26	4.80	40.13	32.96	26.73
	NMF-CC	43.57	30.01	21.44	14.01	6.13	5.08	49.45	35.26	29.08
	UEAF	58.57	47.26	45.68	50.41	32.44	21.98	48.97	43.26	31.07
	UIMC	60.03	47.86	39.94	52.74	30.41	22.86	53.64	42.75	40.39
Our ANIMC	65.75	51.62	47.63	54.27	50.08	25.60	60.02	52.64	49.43	
BUAA	AGC_IMC	72.04	56.80	27.93	78.60	64.99	47.01	74.30	52.60	41.67
	BSV	31.17	26.93	10.86	39.07	30.26	25.01	33.06	20.31	11.48
	Concat	32.09	27.81	13.60	41.07	32.49	26.33	35.12	20.91	13.04
	DAIMC	41.75	38.26	35.53	57.64	50.17	43.10	46.26	39.21	34.52
	EE-IMVC	70.01	57.23	28.07	59.00	50.08	42.66	73.01	51.77	40.04
	EE-R-IMVC	71.08	58.99	30.03	63.71	52.80	45.96	75.99	53.87	40.08
	MIC	34.11	28.33	22.78	50.61	46.89	38.90	40.00	28.87	15.46
	MLAN	34.44	24.06	11.12	36.88	28.19	6.33	36.67	25.56	11.74
	NMF-CC	50.13	39.41	22.41	55.10	51.64	25.11	48.11	41.71	25.01
	UEAF	38.89	31.67	21.08	52.86	42.83	33.86	40.56	37.22	33.33
	UIMC	72.83	60.17	33.96	77.71	65.10	47.93	76.04	58.85	43.07
Our ANIMC	78.23	63.81	40.16	82.07	69.57	51.72	80.06	62.11	50.42	
Caltech7	AGC_IMC	61.83	56.77	51.32	60.76	58.99	52.37	70.42	63.71	64.32
	BSV	44.74	33.61	30.87	47.32	40.87	36.08	66.47	60.83	53.61
	Concat	46.51	35.70	32.18	49.13	42.41	37.80	69.44	61.09	55.72
	DAIMC	51.86	46.33	43.85	56.43	54.17	48.26	73.01	71.18	67.64
	EE-IMVC	61.26	54.97	49.93	61.47	58.93	50.14	76.88	67.43	64.52
	EE-R-IMVC	61.77	55.08	50.16	61.87	59.43	51.08	77.15	67.48	65.72
	MIC	37.52	34.86	27.99	48.53	41.71	35.75	72.33	69.13	60.07
	MLAN	38.01	29.33	19.20	47.62	30.98	21.76	70.42	51.71	37.14
	NMF-CC	39.15	24.84	18.53	49.80	27.91	20.43	68.77	50.38	35.91
	UEAF	62.81	54.88	48.97	61.73	60.01	52.77	78.41	70.80	66.42
	UIMC	64.27	54.40	47.89	60.72	57.38	51.82	77.21	70.49	67.16
Our ANIMC	66.76	56.79	51.73	63.42	62.88	54.71	80.06	74.53	68.72	
Digit	AGC_IMC	85.72	82.66	70.33	80.46	72.89	69.48	84.92	83.08	71.26
	BSV	61.73	54.36	35.72	59.94	50.17	48.73	63.58	56.41	34.55
	Concat	63.15	55.72	37.46	60.73	52.18	50.24	63.77	57.03	35.49
	DAIMC	90.35	87.25	85.05	82.32	77.91	73.31	90.17	87.16	84.89
	EE-IMVC	56.48	49.67	30.76	52.14	48.49	33.62	56.98	40.07	33.89
	EE-R-IMVC	57.06	50.38	33.61	54.82	49.66	34.83	58.72	42.96	35.17
	MIC	52.75	20.90	12.05	45.99	12.30	2.08	52.05	19.60	11.95
	MLAN	19.75	10.21	4.37	14.52	8.71	3.16	23.10	6.04	1.63
	NMF-CC	61.25	59.45	34.90	53.02	47.53	31.59	62.60	56.45	41.93
	UEAF	55.10	38.85	30.42	49.54	37.50	28.32	55.83	40.16	32.55
	UIMC	92.15	88.73	84.62	87.01	78.54	70.88	92.45	84.76	80.24
Our ANIMC	95.00	90.46	85.85	89.48	82.37	73.04	95.13	90.68	85.90	
NH-face	AGC_IMC	79.06	72.83	63.16	68.40	56.73	46.25	78.94	70.12	66.31
	BSV	65.32	54.26	47.38	54.27	36.71	22.84	71.43	57.88	48.26
	Concat	76.57	58.42	50.73	73.45	54.88	44.39	80.43	59.16	48.73
	DAIMC	85.40	80.26	72.71	76.43	70.54	65.82	84.97	80.53	73.88
	EE-IMVC	79.53	69.78	61.54	66.81	53.17	44.06	78.60	69.85	66.13
	EE-R-IMVC	81.75	73.84	64.73	67.48	54.22	45.18	79.14	70.98	67.41
	MIC	74.26	70.50	68.35	70.32	64.59	59.63	80.27	76.40	72.18
	MLAN	52.17	36.02	21.03	50.28	28.91	19.76	53.88	34.96	20.18
	NMF-CC	76.59	70.06	63.84	71.87	68.43	61.80	78.46	77.25	69.43
	UEAF	78.29	70.16	62.35	64.22	51.63	42.81	77.92	71.46	68.20
	UIMC	85.52	80.88	73.79	77.48	70.53	65.59	86.13	81.44	72.96
Our ANIMC	89.05	86.73	85.46	82.47	79.93	76.44	90.47	88.11	87.83	
Scene	AGC_IMC	68.05	60.49	52.47	50.16	43.95	39.56	67.80	50.93	45.16
	BSV	64.88	50.16	43.11	41.60	36.05	29.31	60.18	57.14	45.72
	Concat	65.43	52.86	42.97	45.13	37.26	28.40	61.09	55.17	48.32
	DAIMC	59.48	51.36	47.90	48.36	39.99	30.72	58.13	54.56	47.26
	EE-IMVC	63.08	54.74	51.33	49.86	43.62	37.50	64.06	55.18	48.09
	EE-R-IMVC	65.88	55.06	50.19	49.72	44.03	36.84	66.95	51.46	47.82
	MIC	48.22	29.42	23.79	24.88	8.69	1.56	49.33	32.12	24.43
	MLAN	45.17	24.80	10.92	22.43	12.38	7.52	44.19	28.54	13.06
	NMF-CC	71.53	65.26	59.87	53.24	45.41	42.10	70.36	66.72	57.25
	UEAF	62.38	53.76	49.23	50.40	48.57	39.16	61.73	50.61	44.82
	UIMC	70.89	68.94	65.88	52.04	51.76	40.16	72.15	70.48	62.70
Our ANIMC	78.19	75.57	66.93	57.29	52.38	41.67	78.19	75.57	66.93	

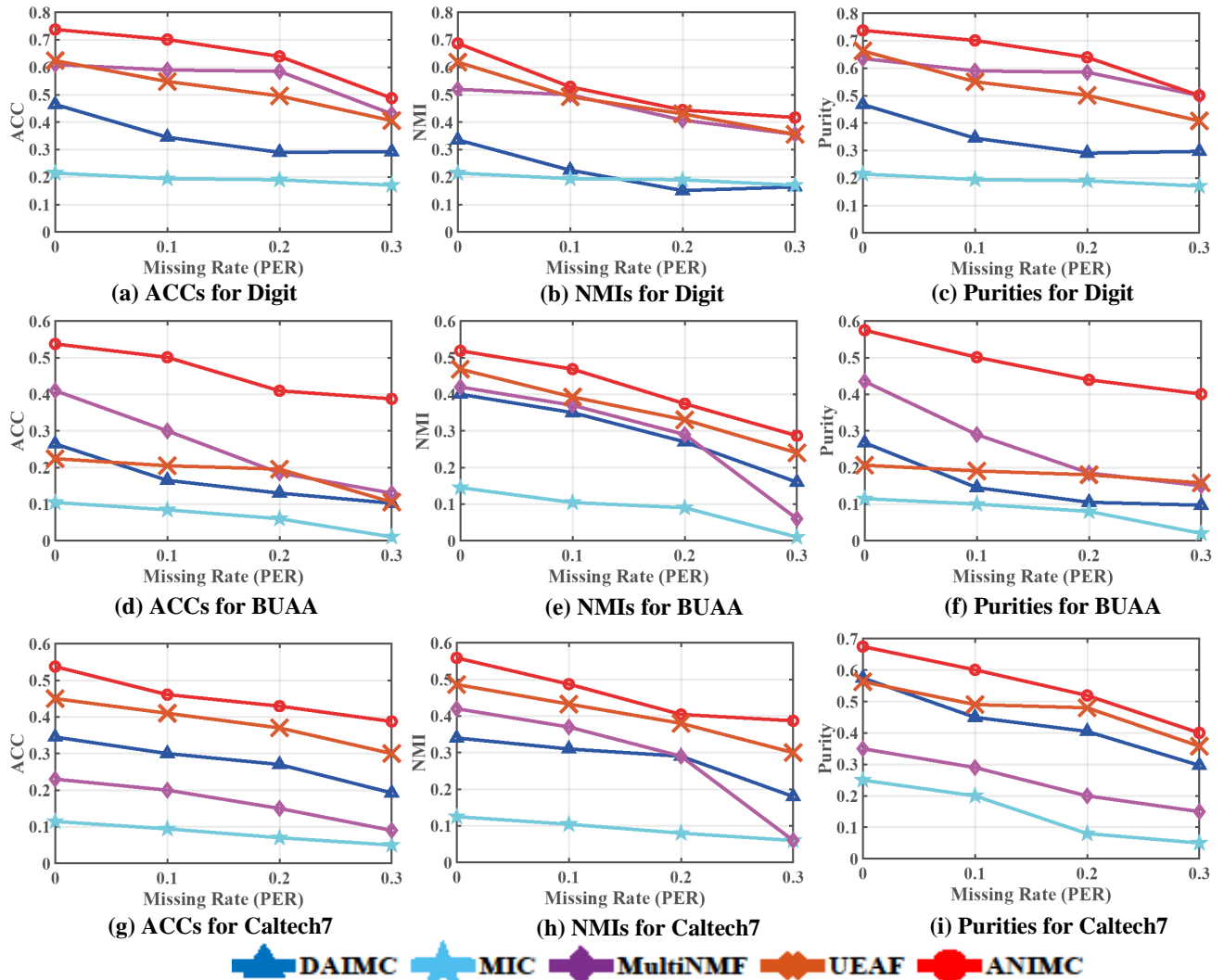


Fig. 2: Noisy and incomplete multi-view clustering on the Digit, BUAA, and Caltech7 datasets.

TABLE III: Performance of our proposed Soft Boundary for noisy and incomplete multi-view clustering on the Digit dataset, where ‘‘ANIMC(SB)’’ denotes our ANIMC with Soft Boundary, ‘‘ANIMC(woSB)’’ denotes our ANIMC without Soft Boundary, and ‘ANIMC(SW)’’ denotes our ANIMC with $w_v = 1$. **Bold** numbers denote the best results.

PER	ACC (%)			NMI (%)			Purity (%)		
	ANIMC(SB)	ANIMC(woSB)	ANIMC(SW)	ANIMC(SB)	ANIMC(woSB)	ANIMC(SW)	ANIMC(SB)	ANIMC(woSB)	ANIMC(SW)
0	73.75	72.63	68.52	68.70	66.09	64.26	73.75	72.03	70.52
0.1	70.10	69.87	67.31	52.87	51.74	47.96	70.10	68.31	65.14
0.2	63.95	60.88	52.94	44.42	40.48	38.92	63.95	60.17	57.64
0.3	48.75	44.93	41.27	41.69	37.61	35.98	50.05	47.35	45.71
0.4	30.67	25.39	21.30	37.26	36.94	33.02	42.19	40.16	39.15
0.5	20.54	13.75	11.06	29.53	28.55	26.69	30.58	28.39	26.71

TABLE IV: Running time (seconds) of different methods for noisy and incomplete multi-view clustering on all datasets (missing rate=0.5, noise rate=0.2, and noise variance=0.1).

Method	BBCSport	BUAA	Caltech7	Digit	NH-face	Scene
AGC_IMC	26.37	43.80	54.71	38.45	107.94	28.76
BSV	9.83	1.04	8.16	6.84	83.54	10.87
Concat	11.27	1.63	10.21	8.74	90.49	12.36
DAIMC	60.88	39.46	27.81	32.94	208.76	52.85
EE-IMVC	65.53	27.31	26.42	48.59	284.76	20.48
EE-R-IMVC	77.24	38.66	19.53	52.87	377.40	15.83
MIC	50.71	16.82	31.60	40.72	384.83	37.15
MLAN	30.18	7.60	6.83	8.64	116.72	25.56
NMF-CC	73.55	10.82	8.54	35.72	120.94	33.67
UEAF	40.96	84.57	43.88	24.50	130.26	30.49
UIMC	31.86	90.85	72.61	20.53	195.47	23.75
Our ANIMC	33.62	51.84	25.06	30.81	174.62	23.18

when PER=0.5, compared with the other methods, MLAN reduces the performance at least about 1.98% in ACC, 0.28% in NMI and 2.35% in Purity, respectively. The main reason is that although it can automatically learn the proper weights for each view from a complete multi-view dataset, MLAN does not effectively integrate incomplete views. Therefore, the self-weighting strategy in MLAN cannot be directly used for incomplete multi-view clustering. Obviously, our proposed ANIMC outperforms all the other methods significantly for various missing rates. Specifically, relative to DAIMC, when the missing rate is relatively small (PER=0.1), ANIMC improves ACC by at least 25.33%, NMI by at least 37.10% and

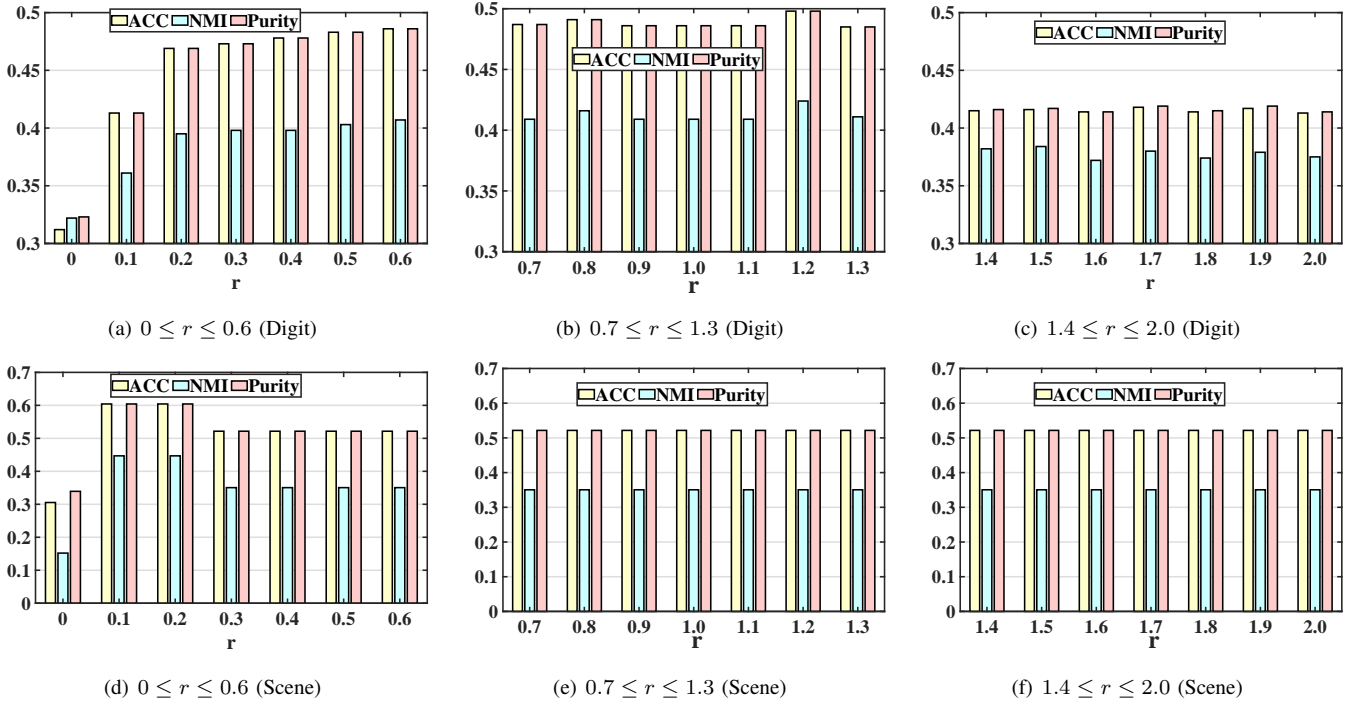


Fig. 3: Noisy and incomplete multi-view clustering on the Digit and Scene datasets with different r .

Purity by at least 18.86%; when the missing rates become larger (PER=0.5), ANIMC still improves ACC by at least 14.16%, NMI by at least 13.97% and Purity by at least 16.52%. One reason for ANIMC’s outstanding performance is that each view of the BBCSport dataset has many features, and ANIMC can effectively integrate these features by minimizing the disagreement between the common latent feature matrix and the common consensus.

BUAA: In the BUAA dataset, DAIMC and UEAF may obtain worse clustering results than other methods. For instance, when PER=0.3, compared with DAIMC and UEAF, NMF-CC raises the performance at least about 1.15% in ACC, 1.14% in NMI and 2.50% in Purity, respectively. This is mainly because the BUAA dataset contains a large number of noises that cause the learned basis matrix $U^{(v)}$ to deviate from the true value, thereby hurting the clustering performance of DAIMC and UEAF. ANIMC performs much better than the other methods for all various missing rates. When PER=0.5, ANIMC raises ACC by at least 4.63%, NMI by at least 3.79% and Purity by at least 7.35%, relative to the compared methods. The reason is that our proposed adaptive semi-RNMF model can assign a smaller weight to the view with more noises (larger deviate for $U^{(v)}$) to efficiently reduce the impact of noises.

Caltech7: Compared with EE-IMVC and EE-R-IMVC, both BSV and Concat perform unsatisfactorily. For example, when PER=0.3, Concat decreases the performance at least about 29.42% in ACC, 17.59% in NMI and 30.86% in Purity, respectively. It is because Concat simply concatenates these views, which makes it difficult to learn consistent information between views.

Digit: As PER increases, the clustering performance of MIC drops significantly. Because MIC only simply fills the missing

samples with average feature values, which will result in a serious deviation for the dataset with high incompleteness. Thus, this simply filling cannot effectively solve the incomplete multi-view clustering problem. Obviously, our proposed ANIMC performs much better than other methods in all cases. Especially, when PER=0.1, compared with AGC_IMC and UIMC, ANIMC improves ACC by at least 2.85%, NMI by at least 2.47% and Purity by at least 2.68%. It is because ANIMC assigns a weight to each view for satisfactory performance.

NH-face: For the dataset, our proposed ANIMC outperforms other methods. For instance, when PER=0.5, ANIMC raises the performance at least about 11.16% in ACC, 10.85% in NMI and 15.14% in Purity, respectively. It is because NH-face has a large number of instances and features, and ANIMC can effectively process these instances and features.

Scene: Obviously, our proposed ANIMC outperforms the other methods in all cases. When PER=0.1, ANIMC raises ACC by at least 7.30%, NMI by at least 4.05% and Purity by at least 6.04%. It is because ANIMC assigns a proper weight to each view thereby decreasing the influence of noises.

D. Noisy and Incomplete Multi-view Clustering

Gaussian noise is one of the most common noises in real-world applications, and many algorithms often use this noise to analyze their de-noising capabilities [125], [126]. In this section, we use the Digit, BUAA, Caltech7 datasets. We add Gaussian noise (noisy rate=0.2, noisy variance=0.1) to these datasets. Before adding noises, we normalize each view matrix of the dataset. Since our proposed ANIMC is based on matrix factorization, we compare ANIMC with NMF-CC, MIC, DAIMC and UEAF, which are also based on matrix factorization.

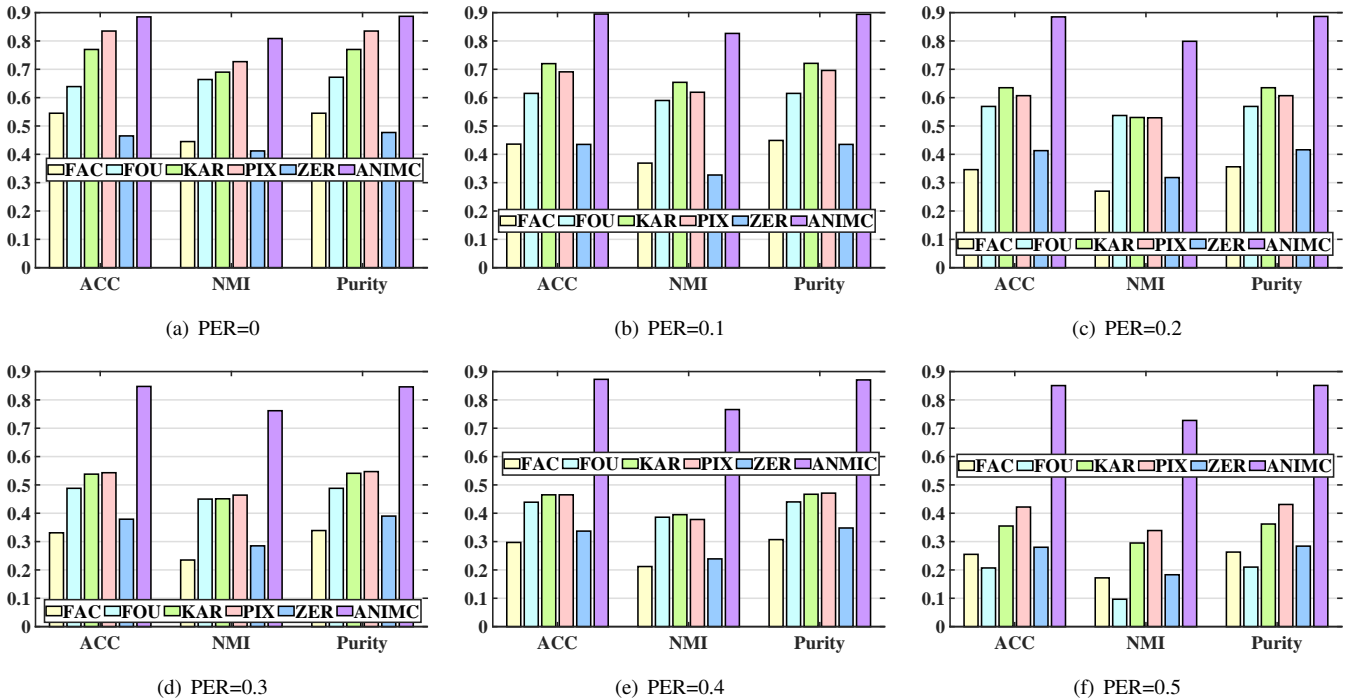


Fig. 4: Availability comparison of different views for incomplete multi-view clustering on the Digit dataset.

Fig. 2 shows the noisy and incomplete multi-view clustering results. Obviously, ANIMC significantly outperforms other methods in all cases. For the Digit dataset with PER=0, compared with these methods, ANIMC raises the clustering performance around 13.52% in ACC and 10.63% in NMI. The outstanding performance of ANIMC verifies its ability to deal with both noises and incompleteness because our adaptive semi-RNMF model can balance the impact of noises and incompleteness based on soft auto-weighted strategy (in Section IV-B). By adaptively assigning a proper weight to each noisy and incomplete view, ANIMC can distinguish the availability of different views for satisfactory performance.

In Table IV, we report the running time of different methods on all the datasets with the missing rate of 0.5, the noise rate of 0.2, and the noise variance of 0.1. We can find that 1) BSV spends the least running time. It is because different from other methods, BSV only deals with the features in one view, which reduces its running time. 2) All methods spend the most running time in the NH-face dataset. The reason is that the dataset has more features and instances, which will increase the running time. 3) In most cases, our proposed ANIMC spends less running time than state-of-the-art UIMC, which shows the efficiency of ANIMC.

Besides, we seek the influence of exponential function with different r , shown in Fig. 3. When we scan it in the whole range (from 0 to 2), the clustering performance keeps a high-level value. Therefore, r is insensitive to the missing rate (PER). Note that when $r = 0$ (i.e., our adaptive semi-RNMF model is removed $w_v \|\mathbf{G}^{(v)} \odot (\mathbf{X}^{(v)} - \mathbf{U}^{(v)} \mathbf{V}^T)\|_F^2 = 0$), the clustering performance is the worst, which validates the importance of the adaptive semi-RNMF model. When $0.2 \leq r \leq 1.3$, ANIMC can obtain relatively good performance. In

our experiments, we choose $r = 0.2$; for θ , we set $\theta = 0.01$ for $\|\mathbf{V}\|_\theta$ and $\theta = 100$ for $\|\mathbf{A}^{(v)}\|_\theta$.

In summary, the performance of all the methods is analyzed as follows. Based on the auto-weighted strategy, MLAN can perform well in complete multi-view clustering tasks. But MLAN is difficult to be directly extended to incomplete multi-view clustering because missing instances will cause the graphs learned by MLAN to be unavailable. As the missing rate increases, the clustering results of both MIC and NMF-CC drop significantly because MIC and NMF-CC neglect the hidden information of the missing instances. Both DAIMC and UEAF rely too much on alignment information. When clustering the dataset without enough alignment information, they always obtain unsatisfactory clustering results because the loss of alignment information will reduce their availability. These drawbacks make these methods difficult to be widely used in real-world applications. By assigning a proper weight to each view via soft auto-weighted strategy and learning the global structure via doubly soft regularized regression model, our proposed ANIMC can obtain satisfactory performance in most cases, which shows that its potential to cluster different real-world datasets well.

E. View Availability Study

To comprehensively analyze the availability of different views, we compare the incomplete multi-view clustering performance of each view on two datasets (Digit and Scene) with different PERs. We compare our proposed ANIMC (multi-view clustering based on ANIMC) with single-view clustering based on ANIMC (e.g., “FAC” in Fig. 4 denotes the clustering performance using ANIMC on view FAC.). The results of the comparison are shown in Fig. 4 and Fig. 5.

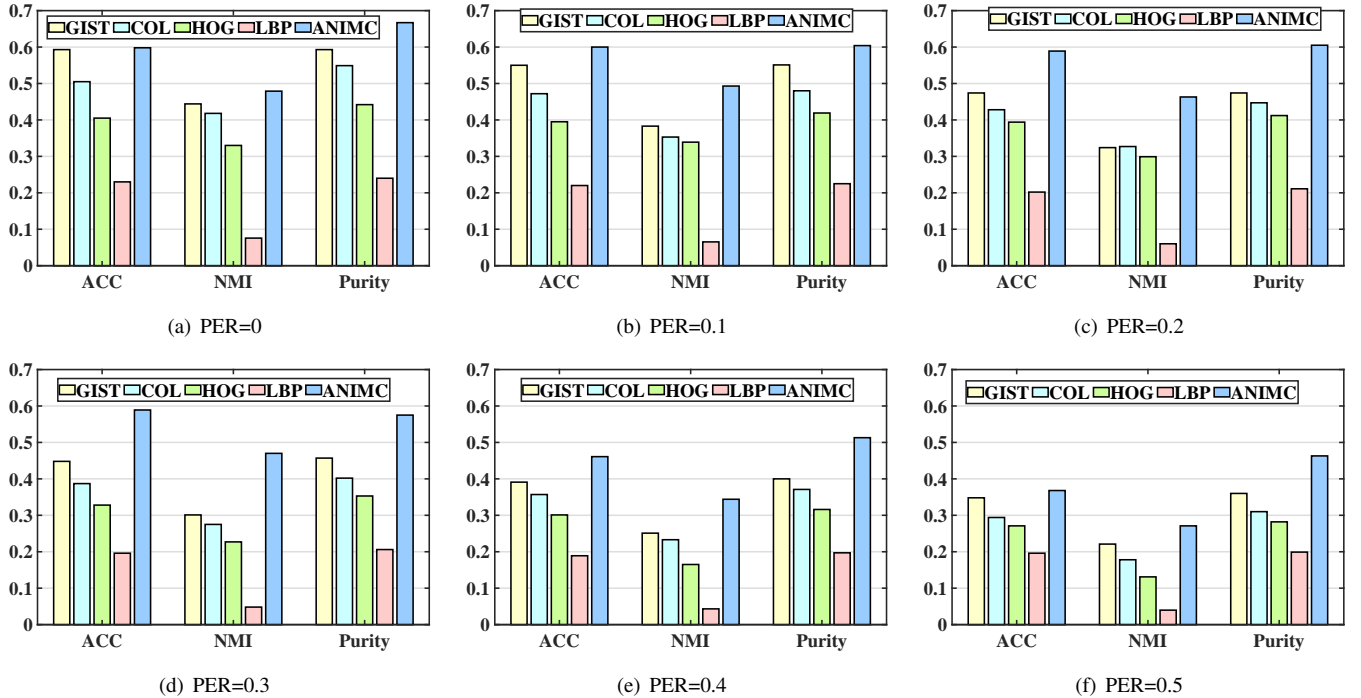


Fig. 5: Availability comparison of different views for incomplete multi-view clustering on the Scene dataset.

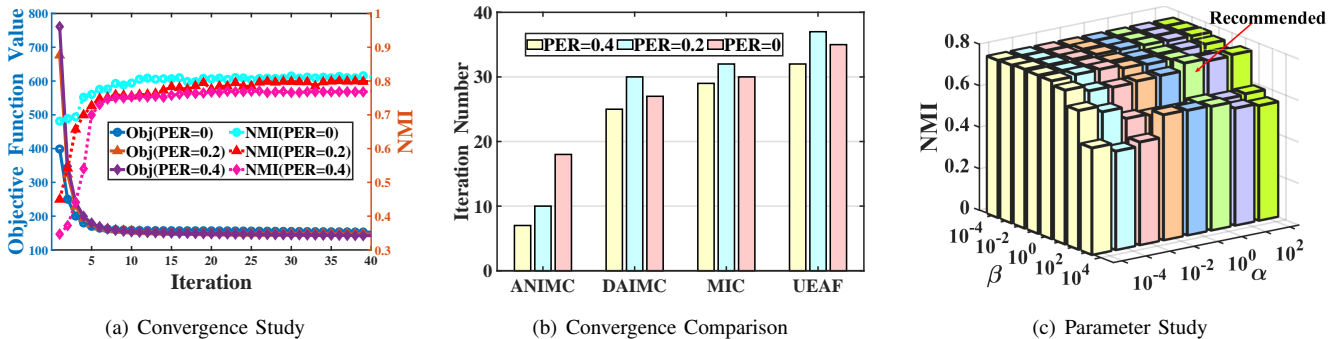


Fig. 6: Convergence and parameter study on the Digit dataset.

Obviously, ANIMC obtains better clustering performance in all cases. For example, when PER=0.5, ANIMC improves ACC by at least 42.90%, NMI by at least 38.80% and Purity by at least 42.01%, which shows that ANIMC can effectively integrate different views for clustering. Moreover, different views have distinct clustering performance on single-view clustering. For instance, KAR and PIX have higher availability than FAC and ZER (see Fig. 4). Besides, as PER changes, distinct views have different relative availability. When clustering the Digit dataset, compared with FAC, FOU can obtain better performance on PER=0 but get worse clustering results on PER=0.5 (see Fig. 4). The comparison of relative availability also shows that we are difficult to choose proper parameters to weight views, which illustrates the significance of our proposed soft auto-weighted strategy (in Section IV-B).

F. Soft Boundary Study

To verify the effectiveness of our soft boundary, we perform experiments to verify the effectiveness of our proposed soft

boundary. In this section, we will compare the performance of our proposed ANIMC with the soft boundary (represented by ANIMC(SB)) and without the soft boundary (represented by ANIMC(woSB)). For ANIMC without soft boundaries, we use Eq. (13) to learn the view weight w_v . For ANIMC with soft boundaries, we use Eq. (14) to obtain w_v . To better demonstrate the effectiveness of our soft auto-weighted strategy, we also compared a popular strategy that all views have the same weight (i.e., $w_v = 1$, represented by ANIMC(SW)). We compared them on the Digit dataset, and report the comparison results in Table III.

As shown in Table III, ANIMC(SW) performs the worst, while ANIMC(SB) obtains the best clustering results in all cases. It is because ANIMC(SW) assigns all views the same weight, which cannot distinguish the importance and availability of each view. This also illustrates the importance of distinguishing the availability of each view. Although ANIMC(woSB) can also distinguish the importance of different views, it cannot measure the impact of noise and incomplete-

ness on each view. Therefore, this method may not be able to obtain satisfactory clustering performance.

G. Convergence Study and Parameter Sensitivity

By perform incomplete multi-view clustering on the Digit dataset, we study the convergence with different PERs, i.e., PER=0, PER=0.2 and PER=0.4. We set the parameters α, β as 0.1, 100, respectively. Also, we set the maximum iteration time $i_{\max} = 40$. Fig. 6(a) shows that the convergence curve and the NMI values versus the iteration number, where ‘‘Obj’’ denotes ‘‘objective function value’’. Note that our proposed ANIMC has converged just after 20 iterations and NMI achieves the best at the convergence point for all PERs. Fig. 6(b) shows the number of iterations when ANIMC, DAIMC, MIC and UEAF converge. ANIMC converges faster than the others. The reason is that ANIMC can make the falling direction of the objective function close to the gradient direction by adaptively learning a proper weight for each view (in Eq. (15)), which shows the efficiency of our proposed soft auto-weighted strategy (in Section IV-B). Especially, when PER increases, the convergence of ANIMC is accelerated. This is because as PER increases, each incomplete view is assigned a larger weight w_v , which increases the difference of the objective function value between before and after each iteration (i.e., the declining rate of the objective function curve increases). Therefore, the objective function can converge to a stable value faster as PER increases.

For different datasets, it is difficult to adaptively select the optimal values for these parameters. Thus, we consider a simple method to obtain the optimal combination of two parameters for experiments. In terms of $\{\alpha, \beta\}$ used in our model, we conduct the parameter experiments on the Digit dataset. Similar to [95], we set PER=0.3 and report the clustering performance of ANIMC versus α and β within the set of $\{10^{-4}, 10^{-3}, 10^{-2}, 10^{-1}, 10^0, 10^1, 10^2, 10^3, 10^4\}$. As shown in Fig. 6(c), ANIMC not only achieves excellent clustering results but also is insensitive to these parameters. Moreover, ANIMC obtains a relatively good performance when $\alpha = 0.1$ and $\beta = 10$. Therefore, we give the recommended values ($\alpha = 0.1$ and $\beta = 10$) and set the recommended values for all the datasets.

VI. CONCLUSION AND FUTURE WORK

In this paper, we propose a novel and soft auto-weighted approach ANIMC for noisy and incomplete multi-view clustering. ANIMC consists of a soft auto-weighted strategy and a doubly soft regularized regression model. On the one hand, the soft auto-weighted strategy is designed to automatically assign a proper weight to each view. On the other hand, the doubly soft regularized regression model is proposed to align the same instances in all views. Extensive experiments on four real-world multi-view datasets demonstrate the effectiveness of ANIMC.

In the future, we will incorporate our approach with deep learning algorithms. By the incorporation, we can effectively deal with the missing instances and noises in a large-scale recommendation system.

REFERENCES

- [1] X. Liu, J. Shi, X. Wu, and G. Zeng, ‘‘Fast first-photon ghost imaging,’’ *Scientific reports*, pp. 1–8, 2018.
- [2] P. Yang, L. Kong, X.-Y. Liu, X. Yuan, and G. Chen, ‘‘Shearlet enhanced snapshot compressive imaging,’’ *IEEE TIP*, 2020.
- [3] X. Fang, Y. Hu, P. Zhou, and D. O. Wu, ‘‘V³h: View variation and view heredity for incomplete multiview clustering,’’ *IEEE TAI*, vol. 1, no. 3, pp. 233–247, 2020.
- [4] A. Blum and T. Mitchell, ‘‘Combining labeled and unlabeled data with co-training,’’ in *COLT*. ACM, 1998, pp. 92–100.
- [5] C. Gong, D. Tao, S. J. Maybank, W. Liu, G. Kang, and J. Yang, ‘‘Multi-modal curriculum learning for semi-supervised image classification,’’ *IEEE TIP*, 2016.
- [6] Q. Tan, G. Yu, J. Wang, C. Domeniconi, and X. Zhang, ‘‘Individuality-and commonality-based multiview multilabel learning,’’ *IEEE Transactions on Cybernetics*, 2019.
- [7] J. Ma, X.-Y. Liu, Z. Shou, and X. Yuan, ‘‘Deep tensor admm-net for snapshot compressive imaging,’’ in *ICCV*, 2019, pp. 10 223–10 232.
- [8] P. Zhou, C. Lu, Z. Lin, and C. Zhang, ‘‘Tensor factorization for low-rank tensor completion,’’ *IEEE TIP*, 2017.
- [9] C. Yan, B. Gong, Y. Wei, and Y. Gao, ‘‘Deep multi-view enhancement hashing for image retrieval,’’ *IEEE TPAMI*, 2020.
- [10] C. Wang, C. Xu, and D. Tao, ‘‘Self-supervised pose adaptation for cross-domain image animation,’’ *IEEE TAI*, vol. 1, no. 1, pp. 34–46, 2020.
- [11] C. Wang, Z. Yan, W. Pedrycz, M. Zhou, and Z. Li, ‘‘A weighted fidelity and regularization-based method for mixed or unknown noise removal from images on graphs,’’ *IEEE TIP*, vol. 29, pp. 5229–5243, 2020.
- [12] D. Liu, X. Fang, W. Hu, and P. Zhou, ‘‘Exploring optical-flow-guided motion and detection-based appearance for temporal sentence grounding,’’ *IEEE Transactions on Multimedia*, vol. 25, pp. 8539–8553, 2023.
- [13] C. Wang, S. He, X. Fang, M. Wu, S.-K. Lam, and P. Tiwari, ‘‘Taylor series-inspired local structure fitting network for few-shot point cloud semantic segmentation,’’ in *Proceedings of the AAAI Conference on Artificial Intelligence*, vol. 39, no. 7, 2025, pp. 7527–7535.
- [14] W. Fang, T. Zhang, W. Tao, and A. Chan, ‘‘Towards understanding modality interaction in multimodal language models via partial information decomposition,’’ in *International Conference on Machine Learning*, 2026.
- [15] M. Kuai, Y. Qin, X. Fang, W. Ji, and R. Zimmermann, ‘‘Dynamic graph-enhanced event refinement for temporal sentence grounding of micro-moments,’’ *IEEE Transactions on Multimedia*, 2026.
- [16] C. Wang, S. He, X. Fang, J. Han, Z. Liu, X. Ning, W. Li, and P. Tiwari, ‘‘Point clouds meets physics: Dynamic acoustic field fitting network for point cloud understanding,’’ in *Proceedings of the Computer Vision and Pattern Recognition Conference*, 2025, pp. 22 182–22 192.
- [17] X. Fang, A. Easwaran, B. Genest, and P. N. Suganthan, ‘‘Your data is not perfect: Towards cross-domain out-of-distribution detection in class-imbalanced data,’’ *Expert Systems with Applications*, 2025.
- [18] X. Zhang, H. Lei, D. Liu, X. Qu, X. Fang, R. Guan, and K. Jin, ‘‘Monoattack: A strong attack framework with depth-migration and attribute-tampering for monocular 3d object detection,’’ in *2025 International Joint Conference on Neural Networks (IJCNN)*. IEEE, 2025, pp. 1–8.
- [19] X. Fang, D. Liu, P. Zhou, Z. Xu, and R. Li, ‘‘Hierarchical local-global transformer for temporal sentence grounding,’’ *IEEE Transactions on Multimedia*, 2023.
- [20] D. Liu, X. Qu, X. Fang, J. Dong, P. Zhou, G. Nan, K. Tang, W. Fang, and Y. Cheng, ‘‘Towards robust temporal activity localization learning with noisy labels,’’ in *Proceedings of the 2024 Joint International Conference on Computational Linguistics, Language Resources and Evaluation (LREC-COLING 2024)*, 2024, pp. 16 630–16 642.
- [21] G. Yang, C. Hou, W. Peng, X. Fang, Y. Nie, P. Zhu, and K. Tang, ‘‘Eood: Entropy-based out-of-distribution detection,’’ in *2025 International Joint Conference on Neural Networks (IJCNN)*. IEEE, 2025, pp. 1–8.
- [22] X. Fang, D. Liu, P. Zhou, and Y. Hu, ‘‘Multi-modal cross-domain alignment network for video moment retrieval,’’ *IEEE Transactions on Multimedia*, vol. 25, pp. 7517–7532, 2022.
- [23] X. Fang, W. Fang, and C. Wang, ‘‘Cogniverse: Revolutionizing multi-modal retrieval-augmented generation with cognitive reflection and geometric reasoning,’’ in *Proceedings of the IEEE/CVF Conference on Computer Vision and Pattern Recognition*, 2026.

- [24] H. Lei, X. Cai, D. Liu, X. Fang, X. Qu, J. Dong, J. Yu, and K. Jin, "Exploring disentangled appearance-motion contexts for temporal activity localization," in *2025 International Joint Conference on Neural Networks (IJCNN)*. IEEE, 2025, pp. 1–8.
- [25] X. Fang, D. Liu, P. Zhou, and G. Nan, "You can ground earlier than see: An effective and efficient pipeline for temporal sentence grounding in compressed videos," in *Proceedings of the IEEE/CVF Conference on Computer Vision and Pattern Recognition*, 2023, pp. 2448–2460.
- [26] C. Wang, X. Fang, and P. Tiwari, "Dypolyseg: Taylor series-inspired dynamic polynomial fitting network for few-shot point cloud semantic segmentation," in *Forty-second International Conference on Machine Learning*, 2025.
- [27] X. Fang, W. Fang, and C. Wang, "Hierarchical semantic-augmented navigation: Optimal transport and graph-driven reasoning for vision-language navigation," in *Advances in Neural Information Processing Systems*, 2025.
- [28] H. Yan, H. Ma, X. Cai, D. Liu, Z. Yuan, X. Qu, J. Dong, R. Guan, X. Fang, H. He *et al.*, "Fit the distribution: Cross-image/prompt adversarial attacks on multimodal large language models," *Advances in Neural Information Processing Systems*, vol. 38, pp. 75 204–75 247, 2026.
- [29] X. Fang, A. Easwaran, and B. Genest, "Adaptive multi-prompt contrastive network for few-shot out-of-distribution detection," in *International Conference on Machine Learning*, 2025.
- [30] C. Wang, S. He, X. Fang, W. Li, Y. Shen, M. Xu, Z. Sun, and P. Tiwari, "Topadapter: Topology-aware prompt tuning for efficient point cloud understanding," *International Conference on Machine Learning*, 2026.
- [31] F. Cai, D. Liu, X. Fang, J. Yu, K. Tang, and P. Zhou, "Imperceptible beam-sensitive adversarial attacks for lidar-based object detection in autonomous driving," in *2025 IEEE International Conference on Multimedia and Expo (ICME)*. IEEE, 2025, pp. 1–6.
- [32] X. Fang and W. Fang, "Slap: The semantic least action principle for variational video-language modeling," in *International Conference on Machine Learning*, 2026.
- [33] C. Wang, S. He, X. Fang, Z. Hu, J.-H. Huang, Y. Shen, and P. Tiwari, "Reasoning beyond points: A visual introspective approach for few-shot 3d segmentation," *Advances in Neural Information Processing Systems*, vol. 38, pp. 117 394–117 414, 2026.
- [34] X. Fang, W. Fang, and W. Ji, "Immuno-vlm: Immunizing large vision-language models via generative semantic antibodies for open-world trustworthiness," in *International Conference on Machine Learning*, 2026.
- [35] C. Wang, Z. Hu, X. Fang, Z. Y. Yu, Y. Wu, M. Xu, Y. Wang, X. Gao, and P. Tiwari, "Biologically-inspired evolutionary domain symbiosis for few-shot and zero-shot point cloud semantic segmentation," in *Proceedings of the AAAI Conference on Artificial Intelligence*, vol. 40, no. 12, 2026, pp. 9666–9674.
- [36] X. Fang and W. Fang, "Disentangling adversarial prompts: A semantic-graph defense for robust llm security," in *Proceedings of the AAAI Conference on Artificial Intelligence*, 2026.
- [37] S. Wang, S. Dutta, W. J. B. Lee, J. Feng, X. Fang, and A. Chattopadhyay, "Reducing t-depth and t-count in quantum multiplication using compressor primitives," in *Proceedings of the Great Lakes Symposium on VLSI 2025*, 2025, pp. 35–40.
- [38] X. Fang, "Advancing out-of-distribution detection across diverse scenarios," in *Proceedings of the AAAI Conference on Artificial Intelligence*, vol. 40, no. 48, 2026, pp. 41 042–41 043.
- [39] X. Fang, W. Fang, and C. Wang, "Unveiling the fragility of vision-language models: Multi-modal adversarial synergy via texture-constrained perturbations and cross-modal optimization," in *Proceedings of the AAAI Conference on Artificial Intelligence*, 2026.
- [40] C. Wang, S. He, X. Fang, W. Li, X. Gao, Z. Liu, P. Tiwari, and D. Kanoulas, "From coarse to fine: Deep prototype refinement network for few-shot point cloud semantic segmentation," *International Conference on Machine Learning*, 2026.
- [41] D. Liu, J. Zhu, X. Fang, Z. Xiong, H. Wang, R. Li, and P. Zhou, "Conditional video diffusion network for fine-grained temporal sentence grounding," *IEEE Transactions on Multimedia*, vol. 26, pp. 5461–5476, 2023.
- [42] D. Liu, X. Cai, J. Dong, Z. Guo, X. Qu, R. Guan, X. Fang, and D. Ye, "Attacking gray-box large vision-language models with adaptive svd-structured adversarial alignment," in *International Conference on Machine Learning*, 2026.
- [43] X. Fang, W. Fang, C. Wang, X. Qu, and D. Liu, "Rethinking video-language model from the language input perspective," in *Proceedings of the AAAI Conference on Artificial Intelligence*, 2026.
- [44] C. Wang, S. He, X. Fang, F. Nan, and P. Tiwari, "Seeing the overlooked: Bio-visual inspired weak saliency feedback transformer for person re-identification," in *Proceedings of the 33rd ACM International Conference on Multimedia*, 2025, pp. 3192–3201.
- [45] X. Fang, W. Fang, C. Wang, K. Tang, D. Liu, S. Wang, and W. Ji, "Towards unified vision-language models with incomplete multi-modal inputs," in *Proceedings of the AAAI Conference on Artificial Intelligence*, 2026.
- [46] X. Fang, W. Fang, C. Wang, D. Liu, K. Tang, J. Dong, P. Zhou, and B. Li, "Multi-pair temporal sentence grounding via multi-thread knowledge transfer network," in *Proceedings of the AAAI Conference on Artificial Intelligence*, vol. 39, no. 3, 2025, pp. 2915–2923.
- [47] X. Fang, D. Liu, W. Fang, P. Zhou, Z. Xu, W. Xu, J. Chen, and R. Li, "Fewer steps, better performance: Efficient cross-modal clip trimming for video moment retrieval using language," in *Proceedings of the AAAI Conference on Artificial Intelligence*, vol. 38, no. 2, 2024, pp. 1735–1743.
- [48] D. Liu, M. Yang, X. Qu, P. Zhou, X. Fang, K. Tang, Y. Wan, and L. Sun, "Pandora's box: Towards building universal attackers against real-world large vision-language models," *Advances in Neural Information Processing Systems*, vol. 37, pp. 52 127–52 158, 2024.
- [49] X. Fang, W. Fang, C. Wang, D. Liu, K. Tang, J. Dong, P. Zhou, and B. Li, "Multi-pair temporal sentence grounding via multi-thread knowledge transfer network," in *Proceedings of the AAAI Conference on Artificial Intelligence*, 2025.
- [50] X. Fang, W. Fang, W. Ji, and T.-S. Chua, "Turing patterns for multimedia: Reaction-diffusion multi-modal fusion for language-guided video moment retrieval," in *ACM International Conference on Multimedia*, 2025.
- [51] X. Fang, W. Fang, D. Liu, X. Qu, J. Dong, P. Zhou, R. Li, Z. Xu, L. Chen, P. Zheng *et al.*, "Not all inputs are valid: Towards open-set video moment retrieval using language," in *Proceedings of the 32nd ACM International Conference on Multimedia*, 2024, pp. 28–37.
- [52] D. Liu, X. Fang, P. Zhou, X. Di, W. Lu, and Y. Cheng, "Hypotheses tree building for one-shot temporal sentence localization," in *Proceedings of the AAAI Conference on Artificial Intelligence*, vol. 37, no. 2, 2023, pp. 1640–1648.
- [53] X. Fang, Z. Xiong, W. Fang, X. Qu, C. Chen, J. Dong, K. Tang, P. Zhou, Y. Cheng, and D. Liu, "Rethinking weakly-supervised video temporal grounding from a game perspective," in *European Conference on Computer Vision*. Springer, 2024.
- [54] D. Liu, X. Fang, X. Qu, J. Dong, H. Yan, Y. Yang, P. Zhou, and Y. Cheng, "Unsupervised domain adaptive temporal sentence localization with mutual information maximization," in *Proceedings of the AAAI Conference on Artificial Intelligence*, vol. 38, no. 4, 2024, pp. 3567–3575.
- [55] X. Fang, D. Liu, W. Fang, P. Zhou, Y. Cheng, K. Tang, and K. Zou, "Annotations are not all you need: A cross-modal knowledge transfer network for unsupervised temporal sentence grounding," in *Findings of the Association for Computational Linguistics: EMNLP 2023*, 2023, pp. 8721–8733.
- [56] Z. Xiong, D. Liu, X. Fang, X. Qu, J. Dong, J. Zhu, K. Tang, and P. Zhou, "Rethinking video sentence grounding from a tracking perspective with memory network and masked attention," *IEEE Transactions on Multimedia*, vol. 26, pp. 11 204–11 218, 2024.
- [57] X. Fang, Y. Hu, P. Zhou, and D. O. Wu, "V3h: View variation and view heredity for incomplete multiview clustering," *IEEE Transactions on Artificial Intelligence*, vol. 1, no. 3, pp. 233–247, 2020.
- [58] J. Wang, J. Li, G. Fan, Y. Ju, X. Fang, and A. C. Kot, "Prototype-driven structure synergy network for remote sensing images segmentation," *IEEE Transactions on Geoscience and Remote Sensing*, 2025.
- [59] X. Zhang, H. Lei, D. Liu, X. Qu, X. Fang, R. Guan, and K. Jin, "Manipulating the bounding box: Multimodal controlled backdoor attacks on 3d visual grounding models," in *2025 International Joint Conference on Neural Networks (IJCNN)*. IEEE, 2025, pp. 1–8.
- [60] W. Fang, T. Zhang, and A. Chan, "To align or not to align: Strategic multimodal representation alignment for optimal performance," in *Proceedings of the AAAI Conference on Artificial Intelligence*, vol. 40, no. 25, 2026, pp. 21 056–21 064.
- [61] K. Tang, W. Zhao, W. Peng, X. Fang, X. Cui, P. Zhu, and Z. Tian, "Reparameterization head for efficient multi-input networks," in *ICASSP 2024-2024 IEEE International Conference on Acoustics, Speech and Signal Processing (ICASSP)*. IEEE, 2024, pp. 6190–6194.
- [62] X. Fang, A. Easwaran, B. Genest, and P. N. Suganthan, "Adaptive hierarchical graph cut for multi-granularity out-of-distribution detection," *IEEE Transactions on Artificial Intelligence*, 2025.

- [63] K. Tang, C. Hou, W. Peng, X. Fang, Z. Wu, Y. Nie, W. Wang, and Z. Tian, "Simplification is all you need against out-of-distribution overconfidence," in *Proceedings of the Computer Vision and Pattern Recognition Conference, 2025*, pp. 5030–5040.
- [64] X. Fang, Y. Hu, P. Zhou, and D. O. Wu, "Unbalanced incomplete multi-view clustering via the scheme of view evolution: Weak views are meat; strong views do eat," *IEEE TETCI*, 2021.
- [65] X. Cai, D. Liu, X. Qu, X. Fang, J. Dong, K. Tang, P. Zhou, L. Sun, and W. Hu, "Towards building model/prompt-transferable attackers against large vision-language models," *Advances in Neural Information Processing Systems*, vol. 38, pp. 174 022–174 058, 2026.
- [66] X. Fang and Y. Hu, "Double self-weighted multi-view clustering via adaptive view fusion," *arXiv preprint arXiv:2011.10396*, 2020.
- [67] Z. Chen and D. Wu, "Prediction of transmission distortion for wireless video communication: Analysis," *IEEE TIP*, 2011.
- [68] D. Shao, Y. Zhao, B. Dai, and D. Lin, "Intra-and inter-action understanding via temporal action parsing," in *CVPR*, 2020, pp. 730–739.
- [69] A. Chambolle, M. J. Ehrhardt, P. Richtárik, and C.-B. Schönlieb, "Stochastic primal-dual hybrid gradient algorithm with arbitrary sampling and imaging applications," *SIAM Journal on Optimization*, 2018.
- [70] W. Min, S. Jiang, S. Wang, J. Sang, and S. Mei, "A delicious recipe analysis framework for exploring multi-modal recipes with various attributes," in *ACM MM*, 2017.
- [71] Z. Liu, S. Wang, L. Zheng, and Q. Tian, "Robust imagegraph: Rank-level feature fusion for image search," *IEEE TIP*, 2017.
- [72] Q.-Y. Jiang and W.-J. Li, "Discrete latent factor model for cross-modal hashing," *IEEE TIP*, 2019.
- [73] P. Zhou, C. Zhang, and Z. Lin, "Bilevel model-based discriminative dictionary learning for recognition," *IEEE TIP*, 2016.
- [74] C. Xu, D. Tao, and C. Xu, "A survey on multi-view learning," *arXiv preprint arXiv:1304.5634*, 2013.
- [75] S. Sun, "A survey of multi-view machine learning," *Neural Computing and Applications*, vol. 23, no. 7–8, pp. 2031–2038, 2013.
- [76] Z. Lu and Y. Peng, "Unified constraint propagation on multi-view data," in *AAAI*, 2013.
- [77] H.-C. Yang, P.-H. Chen, K.-W. Chen, C.-Y. Lee, and Y.-S. Chen, "Fade: Feature aggregation for depth estimation with multi-view stereo," *IEEE TIP*, 2020.
- [78] H. Li, J. Zhang, and C. Zong, "Implicit discourse relation recognition for english and chinese with multiview modeling and effective representation learning," *ACM TALLIP*, vol. 16, no. 3, p. 19, 2017.
- [79] C. Zhang, Q. Hu, H. Fu, P. Zhu, and X. Cao, "Latent multi-view subspace clustering," in *CVPR*, 2017, pp. 4279–4287.
- [80] X. He, Q. Liu, and Y. Yang, "Mv-gnn: Multi-view graph neural network for compression artifacts reduction," *IEEE TIP*, 2020.
- [81] X. Jia, X.-Y. Jing, X. Zhu, S. Chen, B. Du, Z. Cai, Z. He, and D. Yue, "Semi-supervised multi-view deep discriminant representation learning," *IEEE TPAMI*, 2020.
- [82] T. Zhou, C. Zhang, C. Gong, H. Bhaskar, and J. Yang, "Multiview latent space learning with feature redundancy minimization," *IEEE transactions on cybernetics*, 2018.
- [83] Z. Kang, Z. Lin, X. Zhu, and W. Xu, "Structured graph learning for scalable subspace clustering: From single view to multiview," *IEEE Transactions on Cybernetics*, 2021.
- [84] A. Y. Ng, M. I. Jordan, and Y. Weiss, "On spectral clustering: Analysis and an algorithm," in *NIPS*, 2002, pp. 849–856.
- [85] F. Nie, J. Li, X. Li *et al.*, "Self-weighted multiview clustering with multiple graphs," in *IJCAI*, 2017, pp. 2564–2570.
- [86] Z. Kang, X. Lu, J. Yi, and Z. Xu, "Self-weighted multiple kernel learning for graph-based clustering and semi-supervised classification," in *IJCAI*. AAAI Press, 2018, pp. 2312–2318.
- [87] J. Liu, C. Wang, J. Gao, and J. Han, "Multi-view clustering via joint nonnegative matrix factorization," in *ICDM*. SIAM, 2013.
- [88] N. Liang, Z. Yang, Z. Li, W. Sun, and S. Xie, "Multi-view clustering by non-negative matrix factorization with co-orthogonal constraints," *Knowledge-Based Systems*, vol. 194, p. 105582, 2020.
- [89] X.-Y. Liu and X. Wang, "Ls-decomposition for robust recovery of sensory big data," *IEEE TBD*, 2018.
- [90] S. G. Chang, B. Yu, and M. Vetterli, "Wavelet thresholding for multiple noisy image copies," *IEEE TIP*, pp. 1631–1635, 2000.
- [91] H. Zhu and M. K. Ng, "Structured dictionary learning for image denoising under mixed gaussian and impulse noise," *IEEE TIP*, 2020.
- [92] M. El Helou and S. Süsstrunk, "Blind universal bayesian image denoising with gaussian noise level learning," *IEEE TIP*, 2020.
- [93] W. Shao, L. He, and S. Y. Philip, "Multiple incomplete views clustering via weighted nonnegative matrix factorization with $l_{2,1}$ regularization," in *ECMLPKDD*. Springer, 2015, pp. 318–334.
- [94] M. Hu and S. Chen, "Doubly aligned incomplete multi-view clustering," in *IJCAI*, 2018, pp. 2262–2268.
- [95] J. Wen, Z. Zhang, Y. Xu, B. Zhang, L. Fei, and H. Liu, "Unified embedding alignment with missing views inferring for incomplete multi-view clustering," in *AAAI*, vol. 33, 2019, pp. 5393–5400.
- [96] F. Nie, G. Cai, J. Li, and X. Li, "Auto-weighted multi-view learning for image clustering and semi-supervised classification," *IEEE TIP*, 2018.
- [97] J. Gu, G. Wang, J. Cai, and T. Chen, "An empirical study of language cnn for image captioning," in *ICCV*, 2017, pp. 1222–1231.
- [98] X. Zhu, S. Zhang, Y. Zhu, W. Zheng, and Y. Yang, "Self-weighted multi-view fuzzy clustering," *ACM TKDD*, vol. 14, no. 4, pp. 1–17, 2020.
- [99] S. Huang, Z. Kang, and Z. Xu, "Auto-weighted multi-view clustering via deep matrix decomposition," *Pattern Recognition*, vol. 97, p. 107015, 2020.
- [100] S. Shi, F. Nie, R. Wang, and X. Li, "Auto-weighted multi-view clustering via spectral embedding," *Neurocomputing*, vol. 399, pp. 369–379, 2020.
- [101] S.-Y. Li, Y. Jiang, and Z.-H. Zhou, "Partial multi-view clustering," in *AAAI*, 2014.
- [102] H. Zhao, H. Liu, and Y. Fu, "Incomplete multi-modal visual data grouping," in *IJCAI*, 2016, pp. 2392–2398.
- [103] A. J. Smola, S. Mika, B. Schölkopf, and R. C. Williamson, "Regularized principal manifolds," *JMLR*, vol. 1, no. Jun, pp. 179–209, 2001.
- [104] Q. Tao, G.-w. Wu, and J. Wang, "A new maximum margin algorithm for one-class problems and its boosting implementation," *Pattern Recognition*, vol. 38, no. 7, pp. 1071–1077, 2005.
- [105] P. Deng, T. Li, H. Wang, S.-J. Horng, Z. Yu, and X. Wang, "Tri-regularized nonnegative matrix tri-factorization for co-clustering," *Knowledge-Based Systems*, vol. 226, p. 107101, 2021.
- [106] S. Carbonnelle and C. De Vleeschouwer, "Intracluster clustering: an implicit learning ability that regularizes dnns," in *ICLR*, 2020.
- [107] C. H. Ding, T. Li, and M. I. Jordan, "Convex and semi-nonnegative matrix factorizations," *IEEE TPAMI*, vol. 32, no. 1, pp. 45–55, 2010.
- [108] X. Liu, X. Zhu, M. Li, C. Tang, E. Zhu, J. Yin, and W. Gao, "Efficient and effective incomplete multi-view clustering," in *AAAI*, vol. 33, no. 01, 2019, pp. 4392–4399.
- [109] X. Liu, M. Li, C. Tang, J. Xia, J. Xiong, L. Liu, M. Kloft, and E. Zhu, "Efficient and effective regularized incomplete multi-view clustering," *IEEE TPAMI*, 2020.
- [110] W.-J. Li and D.-Y. Yeung, "Relation regularized matrix factorization," in *IJCAI*, 2009.
- [111] S. Gunasekar, B. E. Woodworth, S. Bhojanapalli, B. Neyshabur, and N. Srebro, "Implicit regularization in matrix factorization," in *NIPS*, 2017, pp. 6151–6159.
- [112] M. Qi, T. Wang, F. Liu, B. Zhang, J. Wang, and Y. Yi, "Unsupervised feature selection by regularized matrix factorization," *Neurocomputing*, vol. 273, pp. 593–610, 2018.
- [113] M. R. Hestenes, "Multiplier and gradient methods," *Journal of optimization theory and applications*, vol. 4, no. 5, pp. 303–320, 1969.
- [114] R. H. Bartels and G. W. Stewart, "Solution of the matrix equation $ax+xb=c$ [f4]," *Communications of the ACM*, pp. 820–826, 1972.
- [115] M. R. Hestenes, E. Stiefel *et al.*, "Methods of conjugate gradients for solving linear systems," *Journal of research of the National Bureau of Standards*, vol. 49, no. 6, pp. 409–436, 1952.
- [116] D. C. Sorensen and A. Antoulas, "The Sylvester equation and approximate balanced reduction," *Linear algebra and its applications*, 2002.
- [117] N. J. Higham, *Accuracy and stability of numerical algorithms*. Siam, 2002, vol. 80.
- [118] D. Greene and P. Cunningham, "Practical solutions to the problem of diagonal dominance in kernel document clustering," in *ICML*, 2006, pp. 377–384.
- [119] D. Huang, J. Sun, and Y. Wang, "The buaa-visnir face database instructions," *School Comput. Sci. Eng., Beihang Univ., Beijing, China, Tech. Rep. IRIP-TR-12-FR-001*, 2012.
- [120] A. Monadjemi, B. Thomas, and M. Mirmehdi, "Experiments on high resolution images towards outdoor scene classification," tech. rep., University of Bristol, Tech. Rep., 2002.
- [121] X. Cai, F. Nie, and H. Huang, "Multi-view k-means clustering on big data," in *IJCAI*, 2013, pp. 2598–2604.
- [122] B. Wu, Y. Zhang, B.-G. Hu, and Q. Ji, "Constrained clustering and its application to face clustering in videos," in *CVPR*, 2013, pp. 3507–3514.
- [123] Z. Hu, F. Nie, R. Wang, and X. Li, "Multi-view spectral clustering via integrating nonnegative embedding and spectral embedding," *Information Fusion*, vol. 55, pp. 251–259, 2020.

- [124] J. Wen, K. Yan, Z. Zhang, Y. Xu, J. Wang, L. Fei, and B. Zhang, "Adaptive graph completion based incomplete multi-view clustering," *IEEE Transactions on Multimedia*, 2020.
- [125] G. Yuan and B. Ghanem, " ℓ_0 tv: A sparse optimization method for impulse noise image restoration," *IEEE TPAMI*, 2017.
- [126] M. Elhoseiny, Y. Zhu, H. Zhang, and A. Elgammal, "Link the head to the" beak": Zero shot learning from noisy text description at part precision," in *CVPR*. IEEE, 2017, pp. 6288–6297.